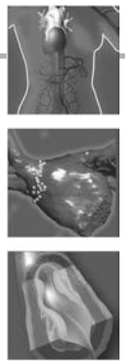

The relationship between plaque imaging characterization and treatment modality selection

It is commonly accepted that knowledge of the degree of luminal stenosis alone is insufficient to predict a plaque's vulnerability. Recently, several imaging techniques, such as high-resolution black-blood magnetic resonance imaging, positron emission tomography/computed tomography, ultrasound, intravascular ultrasound and computed tomography angiography, have emerged that are able to depict the arterial lumen and the vessel wall. This article will describe the potential of these imaging techniques for the identification of vulnerable plaques and will focus on the current evidence that describe the relationship between plaque imaging characterization and treatment modality selection in the coronary and carotid arteries.

KEYWORDS: atherosclerosis ▪ carotid endarterectomy ▪ intravascular ultrasound ▪ MRI ▪ positron emission tomography/computed tomography scan ▪ stenosis ▪ stenting ▪ ultrasound ▪ vulnerable plaque

F Schwarz[1], M Treitl[1], J Grimm[1], C Cyran[1], K Nikolaou[1], M Reiser[1] & T Saam[†1]

[1]Institute of Clinical Radiology, University of Munich, Pettenkoferstr. 8a 80336 Munich, Germany
[†]Author for correspondence:
Tel.: +49 895 160 9285
Fax: +49 895 160 9282
tobias.saam@med.lmu.de

Complications of atherosclerotic disease, namely acute coronary syndrome (ACS) and stroke, are among the leading causes of morbidity and mortality worldwide [1,2]. Atherosclerosis is a chronic disease that remains asymptomatic for decades. However, it is frequently complicated by acute thrombosis, usually triggered by the rupture or erosion of an atherosclerotic plaque, which in turn precipitates the acute ischemic event. Despite major advances in the treatment of atherosclerosis, a large proportion of patients die seemingly healthy and without prior symptoms [3].

There is increasing evidence that the degree of luminal stenosis alone insufficiently predicts the risk of subsequent plaque rupture in various arterial beds [4]. It has been shown that the majority of myocardial infarcts (MI) occur in vessels with less than 50% stenosis (Figure 1) [5,6]. In a large, prospective natural history study of coronary atherosclerosis, Stone *et al.* recently demonstrated that lesions responsible for unanticipated events during the follow-up period were frequently angiographically mild (mean degree of stenosis 32%), most were thin-cap fibroatheromas (TCFAs; as assessed by intravascular ultrasound [IVUS]) or were characterized by a large plaque burden, a small luminal area, or some combination of these characteristics [7].

Recently, the concept of plaque vulnerability or the 'vulnerable plaque' has been put forward. Vulnerable plaques are atherosclerotic plaques that have a high likelihood of causing thrombotic complications, such as myocardial infarction or stroke. Plaques that progress rapidly are also considered vulnerable. On the basis of clinical and pathological evaluation, five major and five minor criteria for plaque vulnerability were recently proposed [5,6]. Major criteria include active inflammation, thrombogenicity, plaque injury, a thin fibrous cap with a large lipid core and severe luminal stenosis. Minor criteria are the presence of calcified nodules, a yellow appearance of the plaque, positive remodeling, intraplaque hemorrhage and endothelial dysfunction.

Despite our advances in understanding the mechanisms of atherosclerotic disease and our knowledge that the degree of luminal stenosis is insufficient to predict a plaque's vulnerability, current imaging markers that are included in the guidelines for carotid and coronary interventions are based solely on the degree of luminal stenosis.

There are several reasons for this paradox:

- Until recently, imaging of the arterial wall was not feasible and the only available imaging marker used in the large clinical trials that validated carotid endarterectomy was the degree of luminal stenosis, as assessed by digital subtraction angiography [8–11];
- It remains a matter of debate which plaque features should be assessed and which imaging modality should be used to assess a plaque's vulnerability;
- Only a limited number of prospective outcome studies with relatively small number of patients based on plaque characterization have been performed;

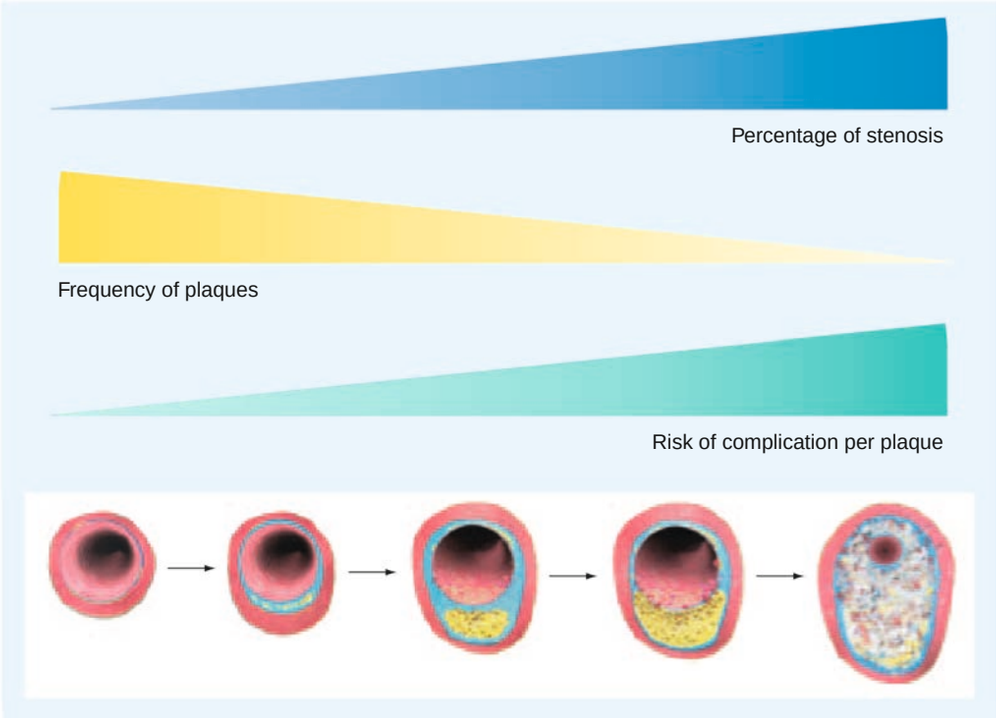

Figure 1. Correlation between percentage of stenosis, frequency of plaques and risk of complication per plaque as a function of plaque progression. Although the average absolute risk of severely stenotic plaques may be higher than the average absolute risk of mildly stenotic plaques, there are more plaques with mild stenoses than plaques with severe stenoses. Reproduced with permission from [5].

- Lack of a representative animal model of plaque rupture and ACS/sudden death.

This article will describe imaging techniques for the identification of vulnerable plaques, such as high-resolution MRI, computed tomography (CT) scan, ultrasound, IVUS and positron emission tomography (PET)/CT scan, and will focus on the current evidence that describe the relationship between plaque imaging characterization and treatment modality selection in the coronary and carotid arteries and other arterial beds.

Imaging techniques for the identification of vulnerable plaques: validation studies

Since the serendipitous invention of invasive coronary angiography by Sones in 1958, a catheter-based approach has been the gold standard for the diagnosis of coronary artery disease [12]. Its main 'product', the invasive coronary angiogram, acquired during direct dye injection, has long been the fundament on which the evaluation of the presence and extent of coronary artery disease (CAD) was built; namely the identification of coronary artery stenoses.

As empirical angiographic data on the natural history of coronary artery disease and its complications became available and pathology extended our understanding of atherosclerotic disease processes within the vessel wall, it became obvious that an assessment of CAD on the basis of luminography (i.e., direct angiography) has major limitations and mostly fails in identifying sites of future plaque rupture and consecutive thrombosis [13].

IVUS

For IVUS, a small ultrasound probe is introduced into the coronary arteries after intracoronary infusion of nitroglycerine and advanced to the most distal part of the vessel [14]. The probe is then automatically retracted ('motorized pull-back') with a speed of 0.5 mm/s while acquiring circumferential ultrasound data that are coregistered with the current intracoronary probe position. An orthograde, cross-sectional image of the coronary artery is displayed to the interventionalist in real-time. For IVUS, high ultrasound frequencies (20–45 MHz) are used resulting in a spatial resolution of approximately 150 µm, typically acquired at frame rates of 10–30 frames/s. IVUS visualizes the coronary artery wall directly and entirely, and thus has the potential to complement the diagnostic information of invasive coronary angiography.

Virtual histology (VH) is a recent extension of IVUS (VH®-IVUS) that applies sophisticated post-processing algorithms of the IVUS raw-data to yield color-coded images of the coronary artery wall that facilitate correlation of images with the histologic profile of plaques [15]. For an intuitive understanding of the plaque composition, IVUS-VH codes four major plaque components in color, namely fibrotic tissue, fibro-fatty tissue, dense calcium and a necrotic core.

IVUS has been extensively validated against histology [16–21]. In patients undergoing directional coronary atherectomy, IVUS-VH has been shown to have a diagnostic accuracy of 87% for the detection of fibrous plaque components, 87% for the fibro-fatty plaque components, 88% for the necrotic core and 96.5% for dense calcium regions [18]. Recently however, the diagnostic accuracy for the detection and quantification of the necrotic core has been challenged by Thim *et al.* who found no correlation between IVUS-VH and histopathology regarding the area of the necrotic core in a porcine model of coronary artery disease [22].

Many plaque features associated with lesion vulnerability are within the scope of this modality, including positive remodeling, hypoechoic plaque components and a spotty pattern of calcification. Assuming that IVUS-VH can image the necrotic core accurately, this modality also permits the visualization of the TCFA. The definition of an IVUS-derived TCFA is a lesion fulfilling the following criteria in at least three frames [7,23]:

- Plaque burden >40%;
- Confluent necrotic core >10% in direct contact with the lumen (i.e., no visible overlying tissue).

It has been known for some time that the high spatial and temporal resolution of IVUS enables direct visualization of plaque or vessel wall damage, such as ulcerations [24], plaque rupture [25], dissection or thrombus formation [25]. Thrombus represents the ultimate pathological feature leading to ACS. Thrombus is usually recognized as an echolucent intraluminal mass, often with a layered or pedunculated appearance by IVUS [26]. Fresh or acute thrombus may appear as an echodense intraluminal tissue, which does not follow the circular appearance of the vessel wall, whilst older, more organized thrombus has a darker ultrasound appearance. However, none of these IVUS features are a hallmark for thrombus, and one should consider slow-flow (fresh thrombus), air, stagnant contrast or black hole, an echolucent neointimal tissue observed after drug-eluting stent and radiation therapy, as differential diagnoses [26]. None of the IVUS-based imaging modalities available can reliably identify thrombus or intraplaque hemorrhage.

■ CT

The quest for higher spatial and temporal resolution, necessary for visualization of rapidly moving coronary arteries has been the number one impetus for innovation in multidetector CT (MDCT) over the last decade. The first tomographic imaging modality with a temporal resolution below 150 ms was electron-beam CT scan and from the beginning, the application of this technique was very much focused on the heart and coronary arteries [27]. Initial efforts were directed towards the visualization of calcium on unenhanced images and different ways of imaging-based calcium quantification were devised (Agatston score; volume score and mass score) [28]. When further technical developments improved temporal resolution in MDCT, this scanner design took the leading role in the field of cardiac CT. In comparison with electron-beam CT, MDCT permits considerably higher photon flux; a prerequisite for CT coronary angiography, particularly in patients with higher body mass.

Today, further improvements in spatial and temporal resolution have turned coronary CT angiography into a routine diagnostic test (Figure 2). The spectrum of patients amenable to noninvasive coronary angiography has been massively extended and now also includes patients with higher heart rates, frequent extrasystoles and atrial fibrillation [29]. A recent systematic review of 18 studies (including 1286 patients) has underlined the excellent diagnostic accuracy of coronary CT angiography on 64-row (or higher) CT scanners for the detection of coronary stenosis >50% (sensitivity: 99%; specificity: 89%; positive predictive value [PPV]: 93%; negative predictive value [NPV]: 100%) [30]. Conversely, in larger multicenter trials the diagnostic accuracy of coronary CT angiography (CTA) noticeably depended on CAD pretest probability in the included patient population, yielding a higher PPV and lower NPV in patients at the higher end of the intermediate risk spectrum (CORE-64) and a lower PPV and excellent NPV at the lower end of the intermediate risk spectrum (ACCURACY).

The introduction of two orthogonally mounted tube-detector arrays (dual-source technology) in 2008, yields a heart-rate independent temporal

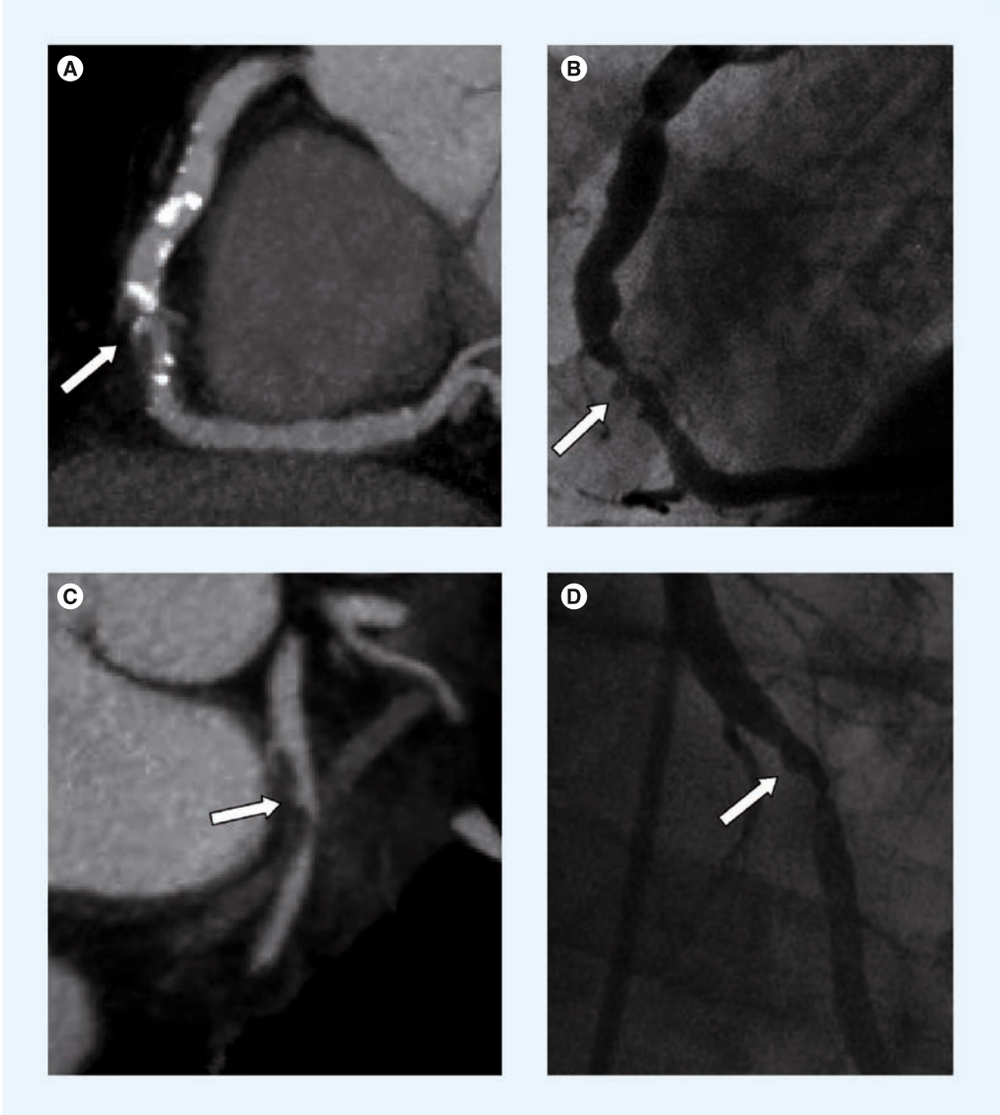

Figure 2. Coronary computed tomography angiography and corresponding invasive angiography of the right coronary artery in a patient with acute chest pain. Small, contrast-filled ulcerations on the plaque surface can clearly be recognized in both modalities.
Reproduced with permission from [98].

resolution of 83 ms [31,32] and also permits novel acquisition techniques such as simultaneous dual-energy acquisition (for which both tubes are operated with different kV-settings) or gapless high-spiral pitch acquisitions (up to a pitch factor of 3.5) with substantial dose reductions [33].

Considerable scientific effort has been directed toward plaque characterization in coronary CTA datasets. In many aspects, CT would seem like the ideal noninvasive modality for this purpose, since it visualizes the coronary artery system quickly, comprehensively and now reaches an isotropic spatial resolution of <0.5 mm at consistently high temporal resolution. Unlike in invasive angiography, all parts of the coronary wall and the surrounding epicardial fat are clearly depicted. Furthermore, different plaque components (calcified, fatty and fibrous) should at least in theory (and in *ex vivo* models) be discernible on the basis of their x-ray attenuation characteristics [34,35], although this is complicated by the fact that brightness of luminal contrast enhancement influences CT scan density values of plaque components [36]. More than spatial resolution itself, contrast resolution between different soft tissue types can become the limiting factor for certain high-risk plaque features, such as the thin-fibrous cap or small, heterogeneously dispersed lipid pools.

Many authors have compared morphologic features of coronary plaques in MDCT with IVUS (Figure 3). Most report significant

differences in mean CT density values for different plaque components as assessed on IVUS [37–42], yet there is uncertainty regarding the degree of overlap of CT density values. While Leber *et al.* [38,39] and Rasouli *et al.* [40] report that plaque components are discernible on the basis of CT values, Pohle *et al.* considered the overlap between different tissue components to be too broad for any distinction [41]. Sun *et al.* found that some plaque components can be differentiated easily (fibrous, fibrous-soft and calcified) while distinction between others is unreliable (soft vs fibrous and soft vs fibrous-soft) [42]. Consistent with this notion, de Weert *et al.* demonstrated a good correlation between MDCT and histopathology in the carotid arteries for plaque volume, calcification and fibrous tissue (r^2 values of 0.73, 0.74 and 0.76, respectively; $p < 0.001$), whereas the correlation for lipid core area was poor ($r^2 = 0.24$; $p = 0.002$). Furthermore, CT is unable to detect intraplaque hemorrhage [43].

With the introduction of VH, IVUS-VH has been used as the reference standard for plaque analysis by MDCT by several groups [44,45]. However, this approach is limited by design, as IVUS itself has difficulties in distinguishing all tissue types. Pundziute *et al.* reported that segmental calcium volume measured by IVUS-VH correlates well with MDCT and plaque classification on MDCT paralleled IVUS-VH [44]. By applying directional coronary atherectomy,

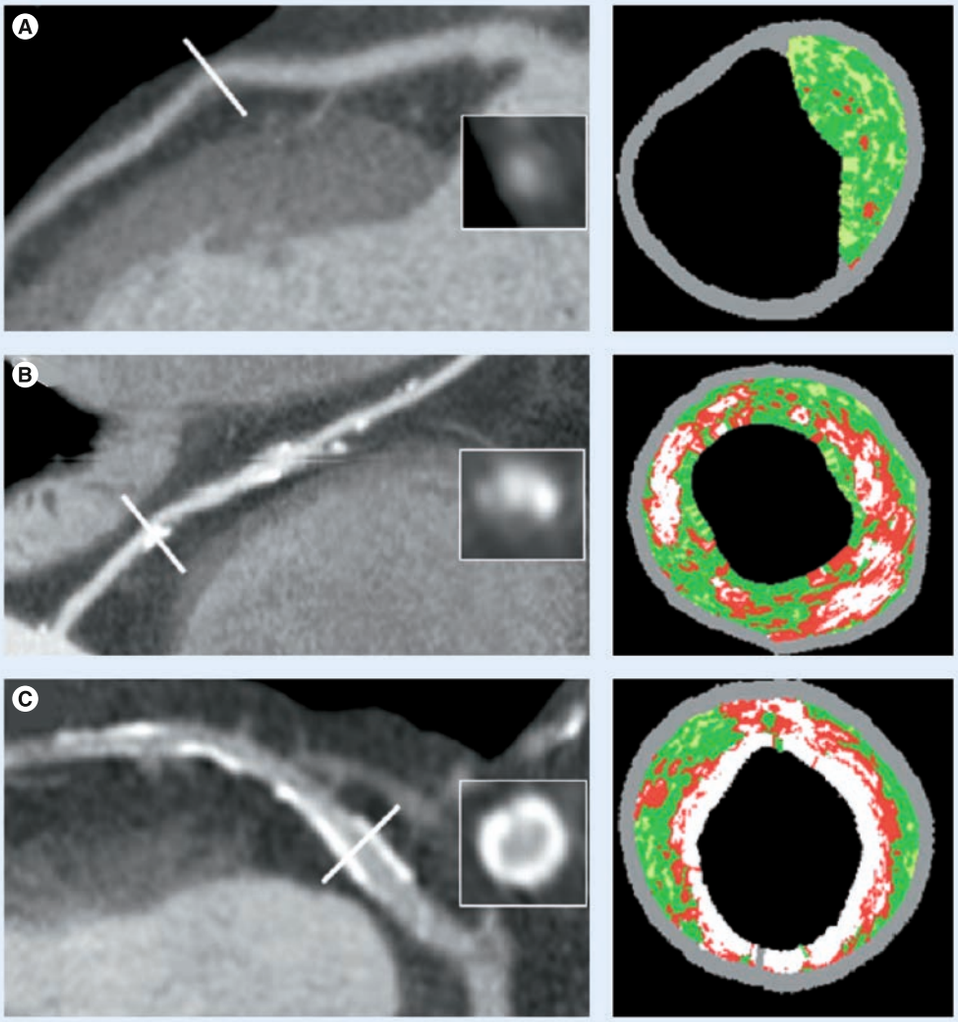

Figure 3. Comparison of orthograde multidetector computed tomography-reformations and intravascular ultrasound-Virtual histology® for the assessment of plaque morphology, exemplified for (A) noncalcified plaque, (B) mixed plaques and (C) calcified plaques.
Components are indicated by dark green for fibrotic tissue; light green for fibro-fatty tissue; red for necrotic core and white for dense calcium.
Reproduced with permission from [44].

Funada *et al.* validated IVUS-VH and MSCT against histopathology and reported difficulties in discerning between different plaque components in MDCT, namely fibrous and fibrous-fatty plaque components [46]. Pedrazzini *et al.* demonstrated that measurements of luminal area stenosis and cross-sectional area by MDCT were in good agreement with those by IVUS, but not by quantitative coronary angiography [47].

With the surge in diagnostic CT scans over the last three decades, radiation exposure and potential cancer induction has become a more widespread concern [48]. When imaging atherosclerotic disease, the risk of cancer induction will not only depend on the technique used, but also on the role of CT imaging within the diagnostic algorithm (i.e., for which patients' CT imaging is applied as a test for atherosclerosis or vulnerable plaques): 65-year old patients will have a much lower risk of radiation-induced cancer than 35-year old patients. Smith-Bindman *et al.* recently calculated that for coronary CT angiography, the attributable lifetime risk for cancer in 40-year old patients is one in 600 men and one in 270 in women [49]. However, the authors assumed a median effective dose of 22 mSv, which exceeds today's industry standards by a factor of at least 4–5. All vendors have put considerable effort in dose reduction, mostly by optimizing scan protocols such as prospective data acquisition, automatic kV- and mAs-adjustments or selective breast-shielding. Another strategy is the optimization of reconstruction algorithms that allow for higher levels of image noise in the raw data set. The main vendors currently strive for CT coronary angiograms with effective doses consistently below 1 mSv, which can by now be achieved in patients with low heart rates and low heart rate variability [50].

Possible future developments in CT scans

Based on distinct absorption characteristics for photons of different energy levels, dual-energy acquisition techniques facilitate material decomposition in CT. For coronary artery plaques this has the potential to improve the visualization of different plaque components [51]. Another interesting concept has been the development of specific contrast agents for CT. In the case of atherosclerosis, this consists of iodine-containing molecules coupled to hydrophobic side chains, resulting in an uptake by macrophages and considerably increasing x-ray attenuation in the plaque. This has recently been demonstrated in a rabbit model by Hyafil *et al.* and validated against histopathology [52,53].

■ MRI

Noninvasive high-resolution black-blood MRI has unique potential to identify the key features of the vulnerable plaque in the carotid arteries(Figure 4 shows exemplary results for different degree of arterial stenosis) [54–57]. MRI is well suited for this role because it is noninvasive, does not involve ionizing radiation, enables the visualization of the vessel lumen and wall and can be repeated serially to track progression or regression. One of the advantages of carotid *in vivo* MRI studies is the possibility of histopathological validation using carotid endarterectomy specimen. Several groups have proven that *in vivo* carotid MRI is able to depict all major plaque components, including the lipid/necrotic core (LR/NC), through unique combinations of signal intensity of each component in different contrast weightings [54–60]. Furthermore, MRI is able to quantify the major components of carotid atherosclerotic plaques with good correlation to histology [59]. MRI measurements of plaque composition were statistically equivalent to those of histology (Figure 5) for the LR/NC (23.7 vs 20.3%; $p = 0.1$), loose fibrous matrix (5.1 vs 6.3%; $p = 0.1$) and dense (fibrous) tissue (66.3 vs 64.0%; $p = 0.4$). Calcification differed significantly when measured as a percentage of wall area (9.4 vs 5.0%; $p < 0.001$), but not in absolute area (2.7 vs 3.5 mm^2; $p = 0.1$). Other studies have demonstrated that MRI is able to determine the presence, the age and the location of plaque hemorrhages [61–63]. Furthermore, MRI is able to identify the fibrous cap, a layer of connective tissue that covers the LR/NC. Lesions with large lipid/necrotic cores and thin, fibrous caps are considered to be most likely to rupture. There are several imaging approaches for MR imaging of the fibrous cap. Hatsukami *et al.* reported the use of a 3D-TOF bright blood imaging technique (multiple overlapping thin-slab angiography [MOTSA]) to identify ruptured fibrous caps in atherosclerotic human carotid arteries *in vivo* [64]. Trivedi *et al.* used a short τ inversion-recovery to quantify the fibrous cap and lipid/necrotic core of 25 recently symptomatic patients and showed good agreement between MRI and histology [56]. Cai *et al.* used T1- and contrast-enhanced-T1-weighted images to measure the intact fibrous cap [65]. The authors showed good correlation between carotid MRI and the excised histology specimen for maximal thickness ($r = 0.78$; $p < 0.001$), length ($r = 0.73$; $p < 0.001$) and area ($r = 0.90$; $p < 0.001$) of the intact fibrous cap. In our opinion, the combination of pre- and postcontrast T1w-, TOF,

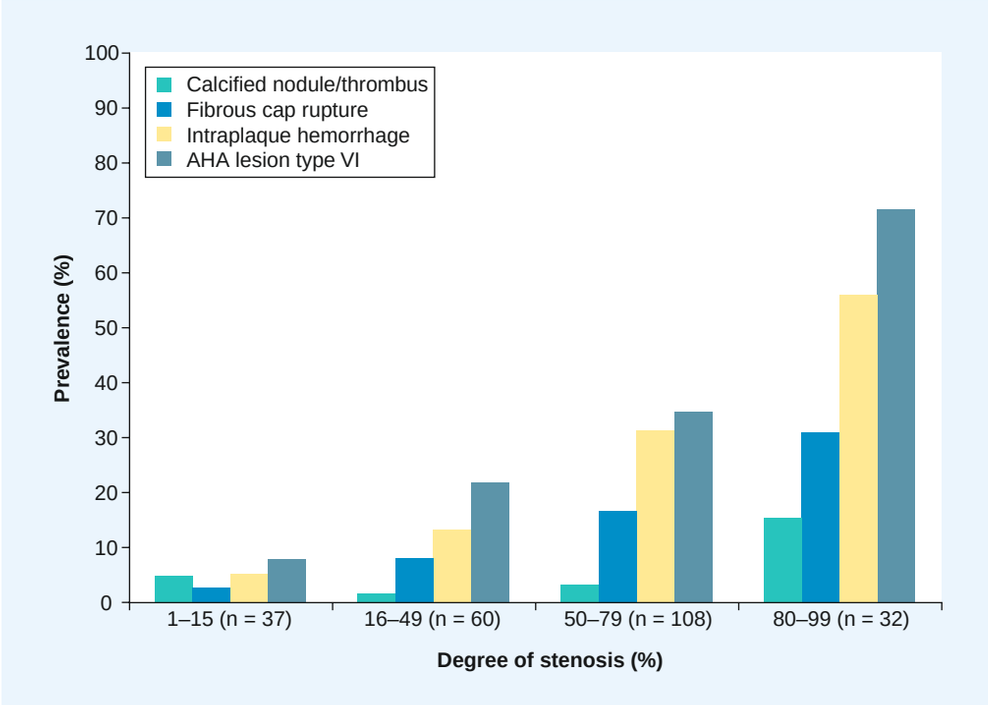

Figure 4. Prevalence of intraplaque hemorrhage, fibrous cap rupture, American Heart Association lesion type VI and other complications (e.g., calcified nodule, calcified plate with juxtaluminal hemorrhage, thrombus and penetrating ulcer) of carotid atherosclerotic plaque in arteries of varying degrees of stenosis as measured by duplex ultrasound.
n = 237 asymptomatic arteries. Of note, one artery could have more than one complication.
AHA: American Heart Association.
Reproduced with permission from [85].

PDw- and T2w- images has the highest potential to identify the fibrous cap and to differentiate between thick, thin and ruptured fibrous cap.

Most imaging of the vessel wall by MRI has been performed at 1.5T scanners. Recently, 3T scanners and their resulting high resolution images have opened the field of vascular imaging to new potentials. These new scanners increase resolution and image quality. A recent study showed signal gains at 3 T relative to 1.5T for carotid artery wall S/N of 223% and wall-lumen contrast-to-noise ratio of 255% in all sequences ($p < 0.025$) [66]. Several recent studies at 3T, some of them using parallel imaging techniques, showed that the number of subjects that have to be excluded due to insufficient image quality can be reduced substantially [67,68]. In our experience with 3 T using parallel imaging techniques, the percentage of nondiagnostic scans is <5%, which is substantially smaller than the number of excluded scans in previous 1.5T MRI studies, where the number of excluded exams ranged from 12 to 33% [57,69,70]. A study by Underhill *et al.* compared the interpretation and quantification of carotid vessel wall morphology and plaque composition at 1.5T with those at 3T MRI in 20 subjects with 16–79% carotid stenosis at duplex ultrasonography [71]. There was a strong level of agreement between field strengths for all morphologic variables, with intra-class

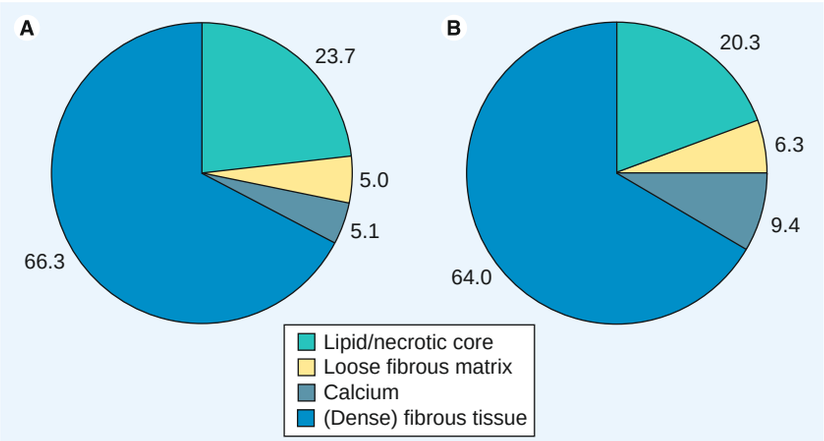

Figure 5. Plaque composition as percentage of vessel wall area, calculated per artery and then averaged across all arteries, for (A) MRI and (B) histologic specimens. Percentages were compared by using paired t-tests. Lipid/necrotic core MRI versus histology: $p = 0.1$; loose fibrous matrix MRI versus histology: $p = 0.01$; calcium MRI versus histology: $p < 0.0001$; (dense) fibrous tissue MRI versus histology: $p = 0.4$.
Reproduced with permission from [59].

correlation coefficients ranging from 0.88 to 0.96. Agreement in the identification of presence or absence of plaque components was very good for calcification ($\kappa = 0.72$), lipid/necrotic core ($\kappa = 0.73$) and hemorrhage ($\kappa = 0.66$). However, the visualization of hemorrhage was greater at 1.5T than at 3T (14.7 vs 7.8%; $p < 0.001$) and calcifications measured significantly ($p = 0.03$) larger at 3T. The authors concluded that at higher field strengths, the increased susceptibility of calcification and paramagnetic ferric iron in hemorrhage may alter quantification and/or detection. Nevertheless, imaging criteria at 1.5T for carotid vessel wall interpretation are applicable at 3T.

MRI is best suited for the study of large or 'static' arteries, such as the carotid arteries. Obviously, the ultimate goal would be noninvasive imaging of coronary artery plaques. Due to their small dimensions and their continuous motion during data acquisition, coronary arteries remain more difficult to image. This is the main reason why most of the data on the detection of vulnerable plaques with MRI have been obtained in large arteries. Fayad *et al.* were the first to demonstrate the feasibility of coronary plaque imaging in humans *in vivo*. MRI of coronary plaques was performed during breath holding in order to minimize respiratory motion [72]. This technique was subsequently improved by Botnar *et al.*, allowing for high-resolution coronary plaque imaging during free breathing. To alleviate the need for breath holding, the black-blood fast-spin echo method has been combined with a real-time navigator for respiratory gating and real-time slice-position correction [73,74]. Near isotropic spatial-resolution black-blood imaging may provide a quick way to image a long segment of the coronary artery wall and may be useful for rapid coronary plaque burden assessment A recent case report by Tanaka *et al.* illustrated the potential of coronary MRI [75]. Figure 6 illustrates a soft coronary plaque on CT images, which is hyperintense on corresponding T1w fat suppressed MR images, indicative of intraplaque hemorrhage. 1 year later, this patient suffered from an ACS due to an occlusion at the site of the previously identified hyperintense lesion on the T1w MR images, suggesting that noncontrast T1w MRI has the potential to identify vulnerable coronary lesions. In the future, further improvement in external coils, as well as the use of contrast agents that enhance the different vessel wall components, may improve MR characterization of the high-risk plaque in the coronary arteries.

■ PET/CT

Inflammation is considered to be one of the key features of vulnerable plaques [5,6]. Pathologic examination of culprit plaques in the victims of acute coronary events reveals extensive infiltration with macrophages; the more macrophages, the thinner the cap [76]. Migration of monocytes to the subintimal layers of the plaque is mediated by expression of receptors for chemoattractant factors such as monocyte chemotactic protein-1 (MCP-1) and those for adhesion molecules such as intercellular adhesion molecule-1 and vascular cell adhesion molecule-1 (VCAM-1) [77]. After subintimal localization, the monocytes express scavenger receptors including SRAI/II, CD68 and FcRIII. Figure 7 demonstrates the molecular principles to detect vulnerable plaques [77]. Whereas multiple candidate targets have been evaluated in preclinical molecular imaging studies, ^{18}F-fluorodesoxyglycose (FDG) and 99 mTc-annexin-A5 appear to be the most promising candidates to image the vulnerable plaque.

^{18}F-FDG imaging for plaque inflammation

A direct correlation between carotid ^{18}F-FDG uptake (expressed as the target-to-background ratio of standardized uptake value) and macrophage density (mean percentage staining of CD68-positive cells) in the carotid endarterectomy specimens has been prospectively demonstrated ($r = 0.85$; $p < 0.0001$) [78]. A FDG-PET study with 216 patients showed an association between the FDG uptake in the carotid arteries and the number of components of the metabolic syndrome, suggesting that the metabolic syndrome is associated with inflammation in carotid atherosclerosis [79]. A recent study in 292 consecutive tumor patients showed that vascular FDG uptake in the coronary arteries could be measured in 161 out of 292 (55%) patients without myocardial uptake [80]. FDG uptake measurements in the left anterior descending artery correlated with hypertension, coronary heart disease, body mass index, pericardial fat volume and the amount of vascular calcification.

Serial prospective ^{18}F-FDG PET studies have reported an excellent interobserver, intraobserver, and interscan reproducibility [81]. The effect of statin intervention on ^{18}F-FDG uptake has been reported in many consecutive patients with carotid atherosclerosis [82]. The follow-up PET scans revealed significant reduction in ^{18}F-FDG accumulation after statin therapy. In this study, only dietary restrictions did not show resolution of vascular inflammation.

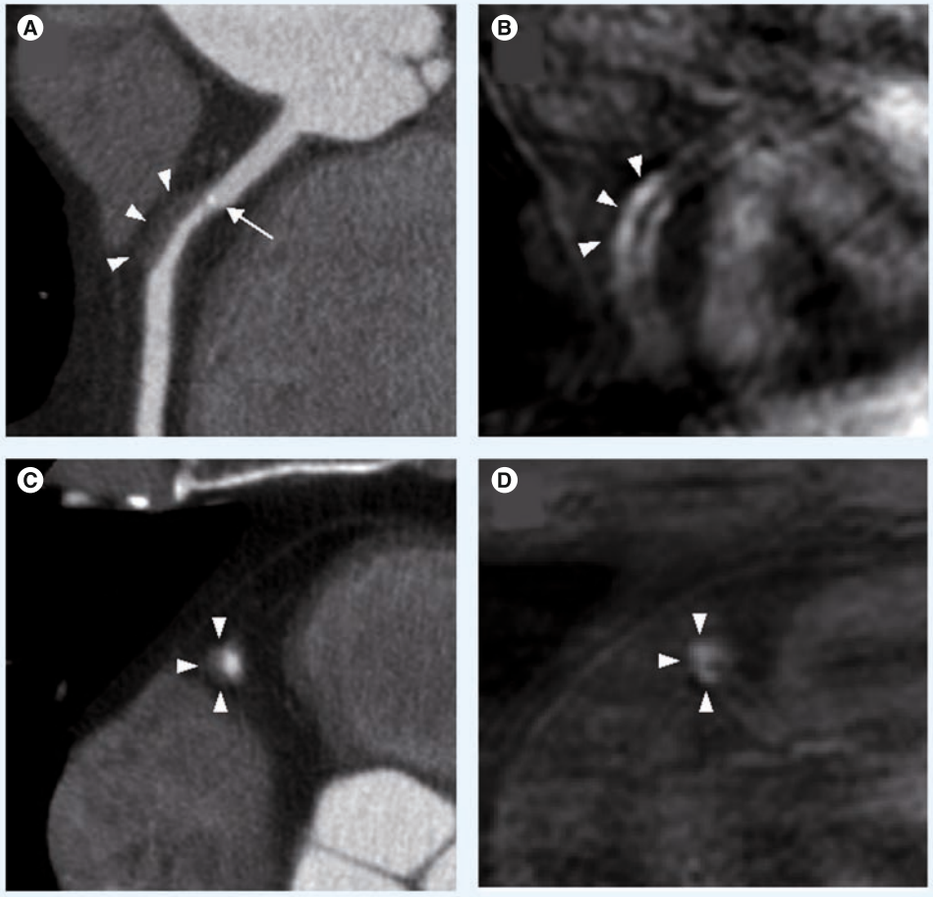

Figure 6. Corresponding multislice computed tomography and magnetic resonance images of coronary artery disease. (A) Curved planar reformat of a contrast-enhanced coronary CT angiography dataset, demonstrating a low-density plaque (-36 Hounsfield units) in the proximal right coronary artery (arrowheads) with spotty calcifications (arrow). Corresponding noncontrast T1-weighted MRI **(B)** shows a hyperintense lesion (arrowheads). **(C)** Demonstrates an axial reformation of the CT dataset. **(D)** An axial MR image of this lesion. 1 year after these examinations, the patient presented with sudden-onset crushing chest pain due to an obstructive lesion in the proximal segment of the right coronary artery in a region corresponding to the hyperintense region previously identified by MRI.
CT: Computed tomography.
Reproduced with permission from [75].

Annexin imaging of atherosclerotic plaques

Because apoptotic cells express phosphatidylserine on their cell surface and AA5 has a high affinity for binding to phosphatidylserine, imaging with 99mTc-labeled AA5 has been used to evaluate the feasibility of the detection of unstable plaques [76]. AA5 has been used previously for noninvasive imaging of experimental atherosclerotic lesions [76,83], and a direct correlation of AA5 uptake with macrophage burden and the magnitude of histologically verified apoptosis was demonstrated.

It should be noted that the PET-component in PET/CT scans comes at a considerable increase in effective dose in comparison with CT scans alone and can therefore not be recommended for routine clinical use for atherosclerosis imaging alone. For ^{18}F-FDG-PET using 370 MBq, the increase in effective dose by the tracer amounts to 6.23 mSv, with particularly high doses in the gonads, uterus and bladder (due to the renal excretion of the tracer) [84].

■ Other imaging techniques

Several other imaging techniques, such as angioscopy, phase contrast imaging, optical coherence tomography, shear stress imaging, near infrared spectroscopy and thermography have been used to assess atherosclerotic plaques [5,6]. Although

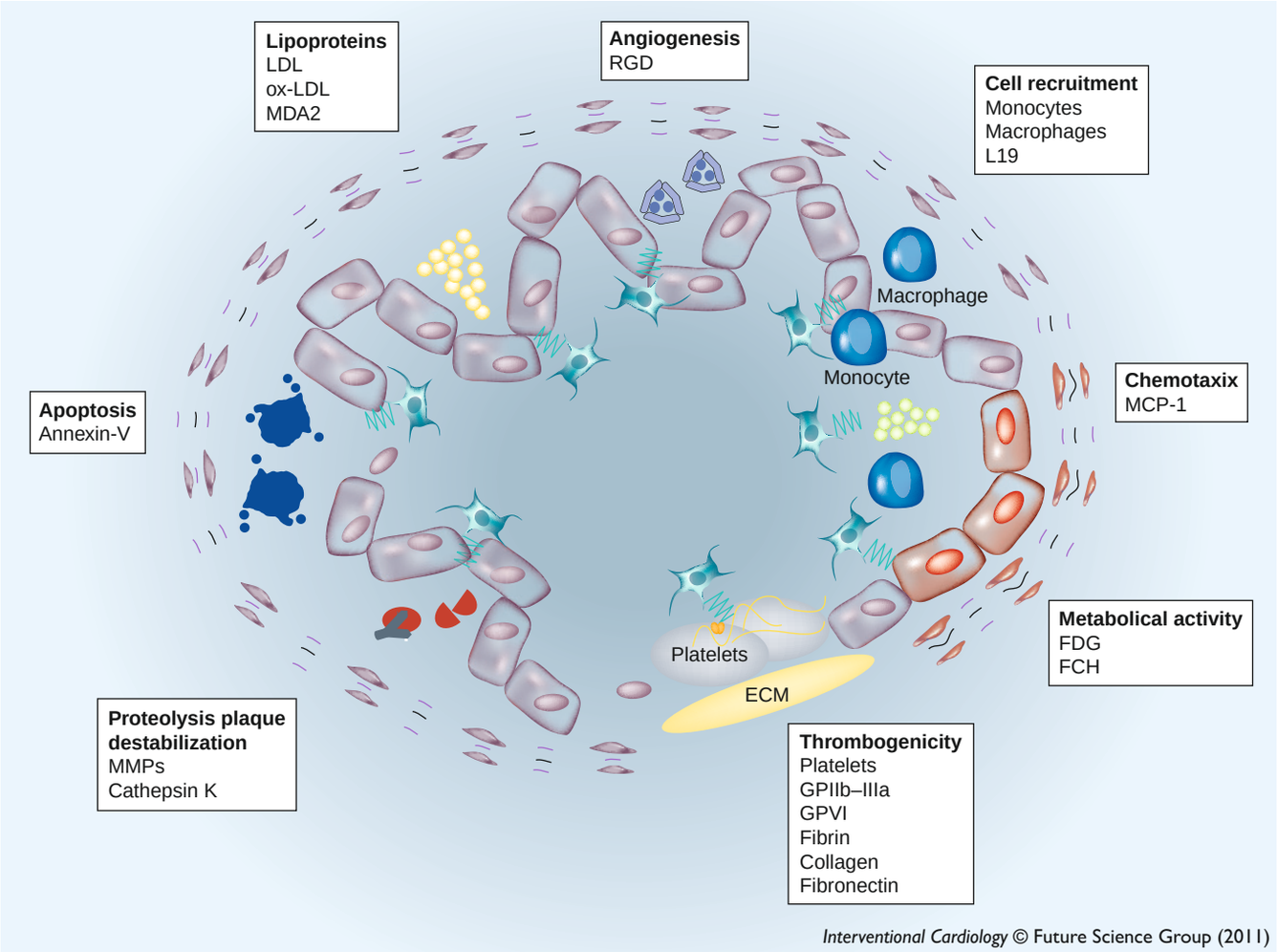

Figure 7. Molecular principles to detect vulnerable atherosclerotic plaques. Based upon the increasing molecular knowledge regarding atherogenesis, different principles have been successfully used to image atherosclerotic plaques. One major complex is the molecular imaging of inflammation, which includes enhanced metabolic activity, chemotaxis, cell recruitment and lipoprotein accumulation. Furthermore, mediators of angiogenesis, apoptosis and matrix metalloproteinase activity have been successfully applied. Another promising approach to detect vulnerable atherosclerotic plaque is the visualization of plaque thrombogenicity, including thrombosis and exposure of thrombogenic subendothelial matrix proteins.
ECM: Extracellular matrix; FCH: Fluorocholine; FDG: Fluorodeoxyglucose; GP: Glycoprotein; L19: Antibody against the extra-domain B of fibronectin; LDL: Low-density lipoprotein; MCP: Monocyte chemoattractant protein; MDA2: Malondialdehyde epitope on ox-LDL; MMP: Matrix-metallo-proteinase; ox-LDL: Oxidized low-density lipoprotein; RGD: Arginine–glycine–aspartic acid.
Reproduced with permission from [77].

many of these techniques are promising, most of them are still under development or not routinely used in clinical routine. Therefore, a detailed analysis of all of these techniques is beyond the scope of this article.

Aim of interventional treatment modalities

Usually luminal stenosis does not by itself cause myocardial infarction or stroke. Ruptures of the fibrous cap expose thrombogenic plaque components to the blood stream inducing luminal thrombus formation. Those thrombi can occlude arteries outright (i.e., coronary occlusion), but more often they detach, move with the bloodstream and eventually occlude smaller downstream branches (i.e., stroke is often caused by thrombus formation in the carotid arteries). Culprit plaques are lesions that have caused an atherosclerotic event. These lesions are highly unstable and need to be treated as soon as possible. They are usually characterized by a ruptured surface that has led to the development of luminal thrombosis. In the coronary arteries these lesions are treated by coronary artery stenting. In the carotid arteries these lesions are treated by carotid endarterectomy or carotid artery stenting if the degree of luminal stenosis is >50%.

It would seem a worthwhile strategy to remove or stabilize vulnerable atherosclerotic plaques

before they can cause thrombotic complications, regardless of the degree of luminal narrowing. Thus, restoration of the luminal diameter would not be the main goal of the intervention, but rather a welcomed side effect. Furthermore, luminal stenosis would not seem to be the ideal parameter to base the decision for intervention on – particularly regarding its limited predictive value for lesion vulnerability. So why is it that we use luminal stenosis as the main imaging criteria for intervention?

Several randomized controlled trials of carotid endarterectomy in asymptomatic and symptomatic patients [8–11] have confirmed the benefit of carotid endarterectomy and clarified those patients most likely to benefit. The benefit varies from an absolute risk reduction of 17% within 2 years with as few as three to six patients undergoing surgery to prevent one stroke (numbers needed to treat) with symptomatic stenosis >70% [8,9], to as little as a 1% absolute risk reduction and 14–17 numbers needed to treat in asymptomatic stenosis >50%. [10,11]. No benefit was observed in patients with stenosis <50% [9]. In the European Carotid Surgery Trial (ECST) [8], benefit was confined to the first 3 years after randomization. Benefit is lost if the complication rate exceeds 3% for asymptomatic and 6% for symptomatic patients. In summary, benefit of the intervention was mainly dependent on the patients´ symptom status and on the degree of luminal stenosis. Figure 8 illustrates why patients with higher degrees of stenosis are more likely to benefit from carotid intervention: with increasing degree of stenosis the corresponding plaques are more likely to have features of complicated plaques. Thus, the degree of luminal stenosis can serve as an indirect marker of plaque vulnerability. This concept was supported by a recent *in vivo* MRI study of 237 asymptomatic arteries with varying degrees of stenosis [85]. Prevalence of complicated American Heart Association type VI plaques was 8.1, 21.7, 35.2 and 71.9% in arteries with 1–15, 16–49, 50–79 and ≥80% stenosis, respectively. However, more than 50% of asymptomatic arteries with >50% stenosis did not have complicated plaques and these patients might not benefit from carotid intervention. In contrast, approximately 16% of asymptomatic arteries with <50% stenosis showed signs of complicated lesions that might benefit from intensive anti-atherosclerotic treatment or surgery. In summary, prevalence of complicated plaques increases with higher degrees of stenosis.

Thus, although the aim of any intervention is to treat vulnerable plaques, the likelihood of a treated plaque being vulnerable is higher in lesions with higher degrees of stenosis. This explains why carotid endarterectomy is more effective in more stenosed vessels.

For the coronary arteries the interventional approach to stenoses has undergone profound changes over the last decade. The landmark trial COURAGE randomized 2287 patients with stable coronary artery disease into two groups: the first underwent best medical therapy only, while the second was also referred for percutaneous coronary intervention and stent implantation [86]. This randomized controlled trial failed to prove a beneficial effect of percutaneous coronary intervention on the risk of death, MI or other major cardiovascular events when combined with optimal medical therapy. Thus, in asymptomatic patients with coronary artery disease, luminal stenosis alone fails to identify subjects who benefit from coronary intervention.

Therefore, it is not surprising that functional parameters such as fractional flow reserve (FFR) turned out to be more successful to base the decision for intervention on. The FAME study randomized 1005 patients with stable coronary artery disease to undergo percutaneous intervention, either on the basis of angiography alone or angiography plus FFR, and showed that in the FFR-group the composite end point of death, nonfatal MI and repeat revascularization at 1 year was significantly (and considerably) lower than in the angiography group (18.3 vs 13.2%) [87].

Plaque imaging & outcome

Over the last two decades, countless studies have attempted to define imaging features associated with plaque vulnerability for several vascular territories. Most were cross-sectional studies, including patients who suffered from an acute event (i.e., MI or stroke) and compared culprit with nonculprit lesions or included a control group with atherosclerotic disease but no acute event. Some studies had a prospective design, including a clinical and imaging follow-up of patients who had undergone some form of plaque imaging. Table 1 shows a list of selected studies that examined the effect of certain plaque imaging features on cerebro- or cardio-vascular events.

■ IVUS & IVUS-VH

Several authors investigated characteristic IVUS-derived plaque features associated with higher lesion vulnerability. As strong parallels exist to plaque features described by CT, details will be discussed together (see below).

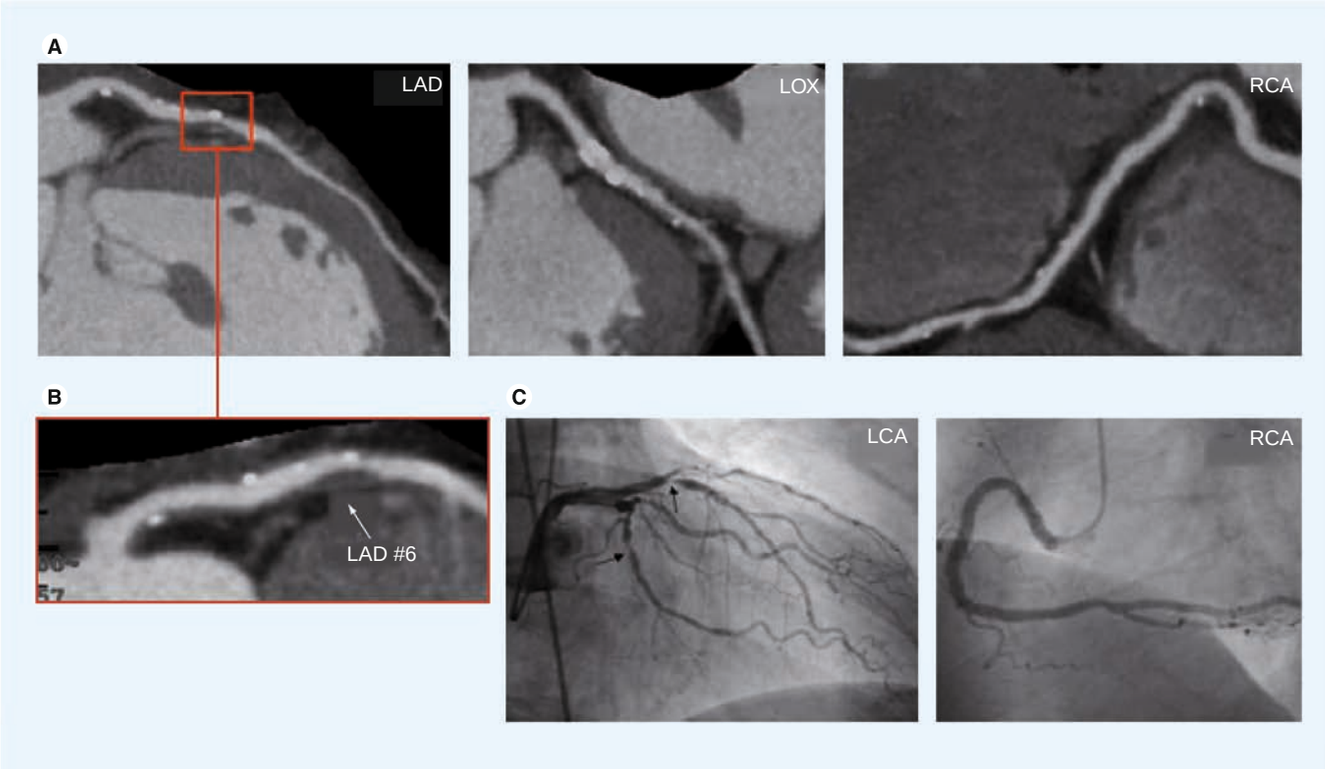

Figure 8. Signs of plaque vulnerability by coronary computed tomography angiography. (A) Curved planar reformat of a coronary CT angiography dataset, showing extensive plaques in the LAD, LCX and RCA. **(B)** Magnification of the proximal LAD region, showing typical signs of plaque vulnerability, such as positive remodelling, low-attention plaque components and spotty calcifications. **(C)** Invasive angiogram on readmission due to an acute infarct 6 months later, showing subtotal occlusion of the proximal LAD.
CT: Computed tomography; LAD: Left anterior descending coronary artery; LCA: Left coronary artery; LCX: Left circumflex artery; RCA: Right coronary artery.
Reproduced with permission from [44].

It should be noted that even in the most modern technical setting, coronary IVUS is associated with a certain risk: in 697 procedures, Stone *et al.* report ten dissections and one coronary artery perforation (complication rate: 1.6%), resulting in three nonfatal MI (0.4%) [7].

■ CT/IVUS

Calcium score

Several studies have analyzed the prognostic value of coronary artery calcium for future cardiac events in symptomatic [88] and asymptomatic [89–92] patients. It has been demonstrated that for the prediction of future cardiac events, the coronary calcium score has incremental prognostic value over established clinical risk scores (e.g., the Framingham risk score [89,91]). If calcium score and clinical risk factors are discordant, calcium has higher prognostic value for future cardiovascular events [93]. Most guidelines recommend coronary calcium screening in patients with intermediate pretest probability for coronary artery disease that can then be reclassified as either high- or low-risk.

Plaque features on CT coronary angiography & IVUS

To investigate which CT scan or IVUS features are associated with an increased risk for plaque rupture and thrombus formation, many authors have analysed culprit lesions in patients who presented with ACS and compared these to either nonculprit lesions or plaques in patients presenting with stable angina pectoris (AP). Currently, prospective data regarding the predictive value of CT-derived plaque features (besides grade of stenosis) for future adverse cardiac events remain scarce [94]. Regarding the predictive value of IVUS-derived plaque features on future cardiac events, there have been a few prospective studies which have attemtped to establish this, including the recently published PROSPECT study [7,95,96].

Several imaging findings are associated with plaque vulnerability, as detailed below.

Larger plaque area/larger plaque volume

Culprit plaques in ACS tend to be larger as measured by plaque area than either nonculprit lesions or lesions in patients with stable AP. For

CT, Hoffmann *et al.* found the average plaque area to be 17.5 ± 5.9 mm² versus 9.1 ± 4.8 mm² in culprit versus nonculprit lesions in patients presenting with ACS [97]. Similar results (for plaques volumes) have been reported by Madder *et al.* recently (313 ± 356 mm³ (culprit) versus 118 ± 93 mm³ [nonculprit] [98]). Motoyama *et al.* demonstrated in a large prospective trial that plaque volume of lesions resulting in ACS was significantly larger than those that did not result in ACS (134.9 ± 14.1 mm³ vs 57.8 ± 5.6 mm³ [94]). Pflederer *et al.* also reported significantly different mean plaque volumes in culprit lesions and stable AP (192.8 ± 14.9 mm³ vs 103.8 ± 51.8 mm³) [99].

For IVUS, most authors report plaque burden as the ratio of plaque area/vessel area. Yamagishi *et al.* found in a prospective study that plaques associated with future ACS during the follow-up period had a higher mean percentage plaque area than those that were not (67 ± 9% vs 57 ± 12%) [96]. Sano *et al.* and Fujii *et al.* reported similar results in cross-sectional studies (60 ± 9% vs 52 ± 9% and 80 ± 8% vs 71 ± 8% vs 69 ± 10% for culprit vs nonculprit vs plaques, respectively in stable AP) [95,100]. Stone *et al.* recently reported in the first results of the PROSPECT study that a plaque burden of ≥70% had a hazard ratio of 5.03 for ACS over the follow-up period of 3 years [7].

Positive remodeling (index)

Several authors reported significantly higher remodeling indexes in culprit lesions versus nonculprit lesions in patients presenting with ACS or versus lesions in patients presenting with stable AP (Hoffmann *et al.*: 1.4 ± 0.3 [culprit lesion] vs 1 ± 0.4 [nonculprit] vs 1.2 ± 0.3 [stable AP] [97] or Motoyama *et al.*: 1.2 ± 0.17 [culprit] vs 0.96 ± 0.12 [stable AP]) [101]. Kröner *et al.* demonstrated that positive remodeling by coronary CT angiography is associated with features of lesion vulnerability by IVUS-VH such as larger necrotic cores (15.7 ± 7.8% vs 10.2 ± 7.2%) and significantly higher rates of TCFA-lesions (43.2 vs 4.8%) [102]. Some authors emphasize that although a positive remodeling index is associated with higher lesion vulnerability, positive remodeling is still quite common in stable plaques [47].

For IVUS, positive remodeling has been described as a feature of vulnerability by multiple studies [25,95,100,103–106], but, interestingly, in the prospective study by Stone *et al.*, the authors did not find a correlation between positive remodeling and vulnerability [7].

High percentage of noncalcified plaques components/low percentage of calcified plaque components (large calcifications)

Culprit lesions in ACS generally have a higher proportion of noncalcified plaque components than nonculprit lesions or lesions in patients with stable AP. Hoffmann *et al.* described noncalcified plaque in 100% of culprit lesions versus 62% of nonculprit lesions and 77% of lesions in patients with stable AP [97]. Similar results are reported by Pflederer *et al.* [99]. Motoyama *et al.* found fewer large calcifications in patients presenting with ACS than with stable AP, but could not detect differences in volumes of intermediate density plaque components (between 30 and 150 HU) [94].

Lower plaque densities/hypoechoic plaque areas (IVUS)/lipid core (VH)

Probably corresponding to more extensive lipid plaque components (lipid core), culprit lesions in ACS generally have lower CT density values than either nonculprit lesions or lesions in patients with stable AP, resulting in a higher frequency of plaques with plaque components <30 HU [101]; a higher area of plaque components <30 HU [94]; a higher ratio of area of plaque with components <30 HU/total area of plaque [94]; a higher volume of plaque components <30 HU [94,98]; lower minimal CT scan values measured within the coronary lesion [99,107]; and lower mean and median plaque densities [99,108].

For IVUS(-VH), plaques associated with ACS were found to have hypoechoic plaque components much more frequently than those that were not by Yamagishi *et al.* [96], Sano *et al.* [95], Kotani *et al.* [25], Missel *et al.* [109], Hong *et al.* [110] and Stone *et al.* [7]. Conversely, Surmely *et al.* report that plaques with positive remodeling did not show an increased frequency of a necrotic core or TCFAs [111]. Recently, the IVUS-VH-based diagnosis of the TCFA has been proposed [23] and is widely applied in several cross-sectional and prospective studies. It should be noted that this relies on an accurate recognition of the presence and extent of a lipid core by IVUS, and has recently been challenged [22].

Spotty pattern of calcification

Although calcification generally shows a negative association with lesion vulnerability, a spotty pattern of calcification (i.e., multiple disseminated calcium speckles within a plaque) shows strong positive correlation with plaque vulnerability (Motoyama *et al.*: 63 [culprit] vs 21% [stable AP] [101]; Pflederer *et al.*: 20 [culprit] vs

Table 1. Exemplary studies analyzing imaging features of plaque vulnerability.

Author (year)	Imaging method	Artery	N	Study design	Outcome (no. of events)	Variable	Results	Ref.
Takaya *et al.* (2006)	MRI	Carotid	154	Prospective	TIA, stroke (12)	Thin/ruptured fibrous cap, intraplaque hemorrhage, mean LR/NC area	OR: 17.0 (95% CI: 2.2–132) OR: 5.2 (95% CI: 1.6–17.2) OR: 1.6 (95% CI: 1.1–2.1)	[114]
Altaf *et al.* (2008)	MRI	Carotid	64	Prospective	TIA, stroke (14)	Intraplaque hemorrhage	OR: 9.8 (95% CI: 1.3–75.1)	[115]
Murphy *et al.* (2003)	MRI	Carotid	120	Cross-sectional	Stroke (120)	Intraplaque hemorrhage/thrombus	More common on the symptomatic side (60 vs 36%)	[113]
Saam *et al.* (2006)	MRI	Carotid	23	Cross-sectional	TIA, stroke (23)	AHA lesion type VI, ruptured fibrous cap, type I hemorrhage	All variables more frequent on the symptomatic side*	[127]
Takaya *et al.* (2005)	MRI	Carotid	29	Longitudinal	Plaque progression	Presence/absence of intraplaque hemorrhage	Accelerated plaque progression in patients with intraplaque hemorrhage (wall volume 6.8 vs -0.15%)	[116]
Rominger *et al.* (2009)	PET/CT	Carotid, aorta, iliac	932	Longitudinal	Vascular events (15)	TBR ≥1.7 vs <1.7 CPS ≥15 vs <15	OR: 14.1 (95% CI: 4.8–41.5) OR: 3.6 (95% CI: 1.2–10.8)	[120]
Rudd *et al.* (2002)	PET/CT	Carotid	8	Cross-sectional	TIA, stroke (14)	FDG uptake	FDG uptake 27% larger on symptomatic side	[118]
Kwee *et al.* (2011)	PET/CT	Carotid	50	Cross sectional	TIA, stroke (50)	FDG uptake (TBR)	TBR significantly larger in the 38 patients which were imaged within 38 days of event (1.24 vs 1.17).	[119]
Rogers *et al.* (2010)	PET/CT	Coronary	25	Cross-sectional	ACS (10)	FDG uptake (TBR)	TBR greater for culprit lesions than for lesions stented for stable coronary syndromes (2.61 vs 1.74).	[128]
Georgiou *et al.* (2001)	CT–CS	Coronary	192	Prospective	MACE or revascularization (58)	CS	Annual event rates: zero calcium: 0.6%, 1–100: 6%, 101–400: 10%, >400: 14%; OR (MACE in patients with any calcium vs zero calcium over 50 months): 28	[88]
Detrano *et al.* (2008)	CT–CS	Coronary	6722	Prospective	MACE (162)	Cs	In comparison with patients without calcium, RR for MACE during follow-up of 3.9 years was 7.7 if CS 101–300 and 9.7 if CS >300	[129]
Pflederer *et al.* (2010)	CTA	Coronary	110	Cross-sectional	ACS (55)	Plaque volume, mean and minimal CT density; RI, plaque type; presence of spotty calcifications	Patients with ACS had higher rates of NCP or mixed plaques with predominance of noncalcified components, higher frequency of spotty calcification, higher RIs, higher plaque volumes and lower mean and minimal CT densities	[99]
Kitagawa *et al.* (2009)	CTA	Coronary	101	Cross-sectional	ACS (21)	RI; frequency of spotty calcification; number of NCP per patient	RI (1.14 vs 1.08), frequency of spotty calcifications (60 vs 38%), number of NCP per patient (3.1 vs 2.0) were higher in ACS than SAP	[107]

*$p < 0.001$.
ACS: Acute coronary syndrome; AHA: American Heart Association; CPS: Calcified plaque score; CS: Calcium score; CT: Computed tomography; CTA: CT angiography; FDG: ^{18}fluorodesoxyglycose; IVUS: Intravascular ultrasound; LR/NC: Lipid-rich necrotic core; MACE: Major adverse cardiac event; NCP: noncalcified plaque; RI: Remodelling index; RR: Risk raio; SAP: Stable angina pectoris; TBR: Target-to-background ratio; TCFA: Thin-cap fibroatheroma; TIA: Transient ischemic attack; VH: Virtual histology.

Table 1. Exemplary studies analyzing imaging features of plaque vulnerability (cont).

Author (year)	Imaging method	Artery	N	Study design	Outcome (no. of events)	Variable	Results	Ref.
Motoyama *et al.* (2009)	CTA	Coronary	1059	Prospective	ACS (15)	RI; plaque volume; volume of low-attenuation plaque components	Patients with positive remodelling and low-attenuation plaques were at a higher risk of ACS developing over time (22.2 vs 0.5%); HR = 22.8	[94]
Madder *et al.* (2011)	CTA	Coronary	60	Cross-sectional	Unstable angina (60)	Plaque volume, RI, volume of low-attenuation plaque	Plaques with features of disruption were more voluminous (313 vs 118 mm³), more often positively remodelled (94.5 vs 44%) and contained more low-attenuation plaques (99 vs 19 mm³)	[98]
Yamagishi *et al.* (2000)	IVUS	Coronary	106	Prospective	ACS (12)	Concentric vs eccentric plaques; mean percentage plaque area	All plaques related to ACS had eccentric pattern and greater percent plaque area (67 vs 57%); frequency of echolucent zones much higher (83 vs 4%)	[96]
Nakamura *et al.* (2001)	IVUS	Coronary	125	Cross-sectional	ACS (54)	Frequency and degress of remodelling; RI	In ACS, frequency and extent of positive remodelling was greater than in SAP (freq = 82 vs 33%; RI = 1.26 vs 0.94)	[104]
Sano *et al.* (2006)	IVUS	Coronary	140	Prospective	ACS (10)	Vessel area; lumen area; plaque area; plaque burden; eccentricity; RI; percentage lipid area; percentage fibrous area	Plaque burden, eccentricity, RI and percentage lipid area were significantly greater in vulnerable than in stable plaques	[95]
Stone *et al.* (2011)	IVUS-VH	Coronary	697	Prospective	MACE (135)	Plaque burden; minimal luminal area; presence of TCFA; RI of nonculprit lesions	Lesions associated with MACE more likely had plaque burden of ≥70% (HR = 5.03) or minimal luminal area of ≤4 mm² (HR = 3.21) or IVUS-TCFA (HR = 3.35)	[7]

*$p < 0.001$.

ACS: Acute coronary syndrome; AHA: American Heart Association; CPS: Calcified plaque score; CS: Calcium score; CT: Computed tomography; CTA: CT angiography; FDG: ^{18}fluorodesoxyglycose; IVUS: Intravascular ultrasound; LR/NC: Lipid-rich necrotic core; MACE: Major adverse cardiac event; NCP: noncalcified plaque; RI: Remodelling index; RR: Risk raio; SAP: Stable angina pectoris; TBR: Target-to-background ratio; TCFA: Thin-cap fibroatheroma; TIA: Transient ischemic attack; VH: Virtual histology.

0% [stable AP] [99]; Kitagawa *et al.*: 60 [culprit] vs 38% [stable AP] [107]). For IVUS, Ehara *et al.* first described that in culprit lesions associated with acute MI, a spotty pattern of calcification was much more common than in nonculprit lesions [106].

Plaque ulceration/thrombus formation

It has been known for some time that the high spatial and temporal resolution of IVUS enables direct visualization plaque or vessel wall damage, such as ulcerations [24], plaque rupture [25], dissection or thrombus formation [25]. Recently, Madder *et al.* have shown that in patients presenting with ACS, features of plaque disruption (such as damage to the endothelial layer and consecutive plaque ulceration) can be visualized by coronary CTA directly and correlate with complex lesions as assessed on subsequent invasive coronary angiography [98].

Comparing IVUS and CT coronary angiography in patients with ACS, Takaoka *et al.* recently demonstrated that CT can distinguish fibrotic coronary plaques from either soft plaques or thrombi, but cannot tell the difference between thrombus and soft plaques [112]. Therefore, the identification and direct visualization of coronary thrombi seems to be restricted to IVUS at present. Since neither of the discussed CT- or IVUS-features is fully sensitive or fully specific for discriminating a coronary artery lesion as vulnerable, several authors calculated relative risks associated for combinations of imaging features. For CT scans, Motoyama *et al.* had compared plaque features of 38 patients presenting with ACS with 33 patients presenting with stable AP and calculated diagnostic performance of different plaque feature combinations for the diagnosis of plaque vulnerability [101]. Subsequently, Motoyama *et al.* followed 1059 patients who had undergone coronary CT angiography for suspected or known CAD for a median observational period of 27 months, and observed that in patients who had coronary artery lesions with positive remodeling and low attenuation components, ACS developed in 22%, while only in 0.5% of patients who showed neither positive remodeling nor low attenuation plaque components [94].

■ MRI

As discussed earlier, carotid high-resolution black-blood MRI (c-hr-bb-MRI) has unique potential to identify intraplaque hemorrhage and the rupture of the fibrous cap. Several cross-sectional studies have shown a higher prevalence of intraplaque hemorrhage/thrombus on the symptomatic compared with the asymptomatic side. Murphy *et al.* showed in a study of 120 symptomatic patients using a T1-weighted fat-suppressed sequence that intraplaque hemorrhages/thrombi are significantly common on the symptomatic side (60 vs 36%; $p < 0.001$) [113].

Parmar *et al.* found a significant association between type VI plaque (demonstrating cap rupture, hemorrhage and/or thrombosis) and ipsilateral transient ischemic attack (TIA)/IS ($p < 0.001$) in 78 acutely symptomatic patients with ischemic stroke or TIA [69]. A multiple logistic regression model, including standard Framingham risk factors and type VI plaque, showed that type VI plaque was the dominant outcome-associated observation achieving significance ($p < 0.001$; odds ratio (OR): 11.66; 95% confidence interval [CI]: 5.31–25.60). The authors concluded that the strong association between type VI plaques and ipsilateral acute TIA/stroke supports the concept that atherosclerosis is the dominant disease pathophysiology in ischemic stroke patients.

A recent prospective *in vivo* MRI study in 154 subjects, who initially had an asymptomatic 50–79% carotid stenosis by duplex ultrasound [114], showed that plaques with intraplaque hemorrhage (hazard ratio: 5.2; 95% CI: 1.6–17.2; $p = 0.004$), thin or ruptured fibrous cap (hazard ratio: 17.0; 95% CI: 2.2–132; $p < 0.001$), larger mean LR/NC area (hazard ratio for 10 mm^2 increase: 1.6; 95% CI: 1.1–2.1; $p = 0.01$) were associated with cerebro-vascular events. Similar to this notion, Altaf *et al.* could show in a prospective study of 64 symptomatic patients with 30–69% carotid stenosis an increased risk of recurrent stroke in patients with intraplaque hemorrhage (OR: 9.8 [95% CI: 1.3–75.1]) [115].

Takaya *et al.* showed in a longitudinal MRI study of 31 patients, that hemorrhage into the carotid plaque accelerated plaque progression over a period of 18 months [116]. The percentage change in wall volume (6.8 vs -0.15%; $p = 0.009$) and lipid/necrotic core volume (28.4 vs -5.2%; $p = 0.001$) was significantly higher in the hemorrhage group compared with the control group. Furthermore, patients with intraplaque hemorrhage at baseline showed a far greater susceptibility to repeat plaque hemorrhages. Therefore, as has been suggested in histological studies and in animal studies, intraplaque hemorrhage may represent a critical transition promoting the

conversion of a stable to an unstable plaque phenotype [117]. In summary, although intraplaque hemorrhage is listed as a minor criteria for the definition of the vulnerable plaque, recent *in vivo* MRI studies suggest a greater role of hemorrhage in plaque destabilization than previously thought.

■ PET/CT

Rudd *et al.* demonstrated in eight subjects with ischemic stroke that FDG uptake was 27% larger on the symptomatic side [118]. Similar to this notion, Kwee *et al.* showed a larger target-to-background ratio in carotid arteries of patients who were imaged within 38 days of event (1.24 vs 1.17; p = 0.014) and a moderate negative correlation between the FDG uptake and the time after symptoms on the side ipsilateral to the ischemic stroke (r = -0.396; p = 0.005) [119]. No significant differences were found in ischemic stroke patients who were imaged more than 38 days after the event, which supports the theory of activated plaques that might have caused the event. In a study of 932 cancer patients it was shown that an increased FDG uptake at baseline and an increased calcified plaque burden, as assessed by PET/CT scans, was associated with an increased risk of future cardio- or cerebro-vascular events [120]. Another PET/CT scan study of the coronary arteries in ten patients with ACS and 15 patients with stable angina showed an increased FDG accumulation both within the culprit lesion as well as in the ascending aorta and left main coronary artery, suggesting inflammatory activity within atherosclerotic plaques in ACS.

The tracer I99mTc-AA5 has been used in a small pilot study for imaging of carotid atherosclerosis in patients with recent or remote cerebro-vascular accidents; AA5 uptake was reported only after recent cerebro-vascular accidents and was not observed in patients being treated with statins. AA5 binding was histologically localized to apoptotic macrophages and also to the red blood cell membranes embedded in necrotic cores. Radiolabeling of AA5 with PET-compatible radiotracers, such as ^{124}I and ^{18}F, is currently under way and may provide better avenues for vascular imaging.

In summary, recent data suggest that FDG uptake is elevated in symptomatic plaques, although the differences between symptomatic and asymptomatic plaques are rather small and seem to disappear within weeks after the event. The study of Rominger *et al.* suggested an increased risk for future cardio- or cerebro-vascular events in patients with elevated FDG uptake at baseline [120].

Plaque imaging & choice of interventional treatment modality

Altaf *et al.* showed, in a study of 60 patients with high-grade symptomatic carotid stenosis undergoing carotid endarterectomy (CEA), that patients with intraplaque hemorrhage as detected by MRI were more likely to have microembolic signals during the dissection phase as measured by transcranial doppler scanning (adjusted OR: 5.8; 95% CI: 1.1–30.4; p = 0.037) [121]. The authors concluded that this imaging technique can be used to identify patients with increased intraoperative thromboembolic risk, and this could influence preventive strategies. Yoshimura *et al.* showed that high-intensity signal (HIS) on TOF MR angiography suggestive of intraplaque hemorrhage indicates carotid plaques at high risk for cerebral embolism after stenting [122]. Ischemic lesions on post-procedural DWI-MRI were more frequent in the HIS-positive plaques (25/38, 65.8%) than in the HIS-negative plaques (26/74, 35.1%; p = 0.006). Periprocedural ischemic symptoms were more frequently observed in HIS-positive plaques (7/38, 18.4%) than in HIS-negative plaques (1/74, 1.4%; p = 0.013). Multivariate logistic regression analysis identified HIS on TOF-MRA as an independent predictor of periprocedural ischemic symptoms (OR: 15.08; 95% CI: 1.76–129.0). Yamada *et al.* performed quantitative analysis of plaque characteristics in carotid arteries using black-blood-MRI before and DWI-MRI after carotid artery stenting (CAS) in 50 patients [123]. In the patient group that was positive (n = 19) for newly appearing ipsilateral silent ischemic lesions (NISIL), signal intensity ratios from T1-weighted images (1.40 ± 0.19 and 1.18 ± 0.25; p < 0.01) were higher than in the NISIL-negative group (n = 31). The same group performed CAS in 56 patients and CEA in 25 patients and showed that in the group with high SIR on black-blood MRI, the incidence of NISIL was significantly greater after CAS than after CEA (61 vs 13%, respectively; p = 0.006), whereas there were no significant difference in NISIL after the two procedures when the SIR was <1.25 (21 vs 0%). In multivariate regression analysis, the independent predictors of NISIL were CAS (p = 0.002), symptomatic stenosis (p = 0.036) and the SIR (p = 0.049). In summary, recent studies suggest that intraplaque hemorrhage, as detected by black-blood MRI,

is associated with an increased risk of CAS. Further studies are needed to determine whether these patients will have lower event rates with carotid endarterectomy.

Currently, there are two strategies for managing patients after the identification of a TCFA. The conservative approach is based on the premise that as long as the PPV and NPV of these imaging techniques for future clinical events has not been established, no local treatment is warranted [124], which is today's standard of care.

At the same time, some studies are underway that test if vulnerable plaques can be intervened on pre-emptively. In the randomized controlled trial Santorini Criteria for Investigating and Treating Thin Capped Fibroatheroma (SECRITT I), 30 patients with 40–50% stenosis and imaging findings of lesion vulnerability but preserved FFR, are randomized to either receive best medical therapy (which is the current standard treatment) or to receive intervention using a self-expanding coronary stent (vProtect® Luminal Shield) [124].

Conclusion

Current studies, although many of them limited by nonrandomized study design, small sample size and short-term follow-up were able to identify certain plaque characteristics that are associated with an increased risk of cardio- or cerebro-vascular events. Of the imaging techniques used to identify the vulnerable plaque, MRI has the highest potential in the carotid arteries, as it has, compared with ultrasound and CT scan, superior soft tissue contrast and is the only imaging modality that can reliably identify intraplaque hemorrhage, one of the key features of vulnerable plaques. PET/CT scan has recently emerged as a viable tool to measure plaque inflammation and several molecular targets have been identified that could be useful to characterize rupture-prone vulnerable lesions. In the coronary arteries, IVUS and CT angiography seem to be promising tools to identify vulnerable lesions. Several imaging markers have been identified that are associated with an increased risk of cardio- or cerebro-vascular events, such as (calcified) plaque burden, intima–media thickness, presence of a thin cap fibroatheroma, echolucent plaques, intraplaque hemorrhage, presence of a thin/ruptured fibrous cap and plaque inflammation. To date, it is not clear which of these imaging markers is best suited to identify vulnerable lesions and further prospective studies are needed that combine new imaging techniques, laboratory and clinical markers to identify the best approach in each individual patient.

Future perspective

Despite extensive studies and the development of several risk prediction models, traditional risk factors, in combination with the degree of luminal stenosis, fail to predict the development of cardio- or cerebro-vascular disease in up to 50% of cases [6]. Noninvasive imaging modalities have the potential to better stratify patient's individual risk according to the morphology of atherosclerotic plaques. These plaque characteristics might then help identify which patients would benefit most from interventional therapy or from a more conservative, medical approach.

Further clinical and epidemiological research is needed to define the optimal role that advanced imaging techniques can play in the workup of atherosclerosis. In this arena, imaging will have to stand next to highly sophisticated laboratory tests detecting the tiniest amounts of proteins or microRNAs as biomarkers. Within a decade or two, high-throughput DNA sequencing will most probably allow for whole-genome sequencing in almost every patient. It will be exciting to see how all these diagnostic components will fit in to further optimize diagnostic algorithms.

While awaiting results of the SECRITT I trial that base the decision for coronary intervention on plaque vulnerability [124] and of the BioImage Study exploring a host of different biochemical and imaging biomarkers for the prediction of subsequent atherosclerotic complications [125], one must acknowledge that there still is a long road ahead until it can be safely decided which lesions require prompt intervention and which can be left alone [126]. If, in the future, the treatment of vulnerable plaque favorably modifies the outcome of patients, vulnerable plaque imaging will not be an elusive goal.

Financial & competing interests disclosure

The authors have no relevant affiliations or financial involvement with any organization or entity with a financial interest in or financial conflict with the subject matter or materials discussed in the manuscript. This includes employment, consultancies, honoraria, stock ownership or options, expert testimony, grants or patents received or pending, or royalties.

No writing assistance was utilized in the production of this manuscript.

Executive summary

Current status

- It is commonly accepted that in atherosclerotic disease the degree of luminal stenosis insufficiently predicts the risk of severe thrombotic complications (myocardial infarct, stroke).
- However, therapeutic decisions are still mostly based on the presence and extent of luminal stenosis.
- Recently, several imaging methods have emerged that allow the depiction of the full vessel wall with high resolution.

Current diagnostic modalities for plaque characterization: intravascular ultrasound/virtual histology

- Very high spatial and soft-tissue (contrast) resolution, but invasive procedure, no first-line test.
- Intravascular ultrasound/virtual histology can differentiate plaque components that have been associated with plaque vulnerability (thin cap fibrous atheroma, spotty calcification, luminal thrombus).
- Substantial evidence in favor of a predictive value of plaque analysis by intravascular ultrasound/virtual histology (multicenter studies).

Current diagnostic modalities for plaque characterization: computed tomography

- High spatial and temporal resolution, noninvasive test, useful for initial evaluation.
- Predictive value of coronary calcium score for future major adverse cardiac events well established.
- Computed tomography coronary angiography now feasible in almost all patients; high-quality datasets provide additional information about plaque vulnerability (degree of luminal stenosis, hypodense plaque components, spotty calcifications, positive remodelling).

Current diagnostic modalities for plaque characterization: MRI

- For the carotid arteries using dedicated surface coils and high-resolution black-blood techniques.
- For detailed plaque characterization multisequence protocols should be used, including time of flight-, pre and postcontrast T1-weighted-, proton-density- and T2-weighted-sequences.
- Noninvasive, very high spatial and soft-tissue contrast resolution, no ionizing radiation involved, ideal for regular follow-up exams.
- There is a high level of evidence in favor of a predictive value of plaque analysis by MRI for the carotid arteries.

Current diagnostic modalities for plaque characterization: ^{18}-fluorodesoxyglycose positron emission tomography

- Can contribute information about the presence and extent of inflammation within the vessel wall and perivascular tissue.
- There is some evidence in favor of a predictive value of high Flurodoxyglucose uptake, however, more prospective trials are needed.
- Currently ^{18}-fluorodesoxyglycose positron emission tomography is not approved for this indication in the USA or Europe and existing studies have mostly been performed in patients who underwent scanning for a noncardiovascular indication.

Conclusion

- Today, several imaging modalities are in place to address plaque vulnerability – large, prospective trials are needed to analyze whether beyond improving the prediction of future events, treatment decisions on the basis of plaque vulnerability also lead to better outcomes.

Bibliography

1 Lloyd-Jones D, Adams RJ, Brown TM *et al.* Executive summary: heart disease and stroke statistics-2010 update: a report from the American Heart Association. *Circulation* 121(7), 948–954 (2010).

2 Lopez AD, Mathers CD, Ezzati M *et al.* Global and regional burden of disease and risk factors, 2001: systematic analysis of population health data. *Lancet* 367(9524), 1747–1757 (2006).

3 Virmani R, Kolodgie FD, Burke AP *et al.* Lessons from sudden coronary death: a comprehensive morphological classification scheme for atherosclerotic lesions. *Arterioscler. Thromb. Vasc. Biol.* 20(5), 1262–1275 (2000).

4 Pasterkamp G, Schoneveld AH, Van der Wal AC *et al.* Relation of arterial geometry to luminal narrowing and histologic markers for plaque vulnerability: the remodeling paradox. *J. Am. Coll. Cardiol.* 32(3), 655–662 (1998).

5 Naghavi M, Libby P, Falk E *et al.* From vulnerable plaque to vulnerable patient: a call for new definitions and risk assessment strategies: part II. *Circulation* 108(15), 1772–1778 (2003).

6 Naghavi M, Libby P, Falk E *et al.* From vulnerable plaque to vulnerable patient: a call for new definitions and risk assessment strategies: part I. *Circulation* 108(14), 1664–1672 (2003).

7 Stone GW, Maehara A, Lansky AJ *et al.* A prospective natural-history study of coronary atherosclerosis. *N. Engl. J. Med* 364(3), 226–235 (2011).

8 MRC European carotid surgery trial: interim results for symptomatic patients with severe (70–99%) or with mild (0–29%) carotid stenosis. European Carotid Surgery Trialists' Collaborative Group. *Lancet* 337(8752), 1235–1243 (1991).

9 Beneficial effect of carotid endarterectomy in symptomatic patients with high-grade carotid stenosis. North-American Symptomatic Carotid Endarterectomy Trial Collaborators. *N. Engl. J. Med.* 325(7), 445–453 (1991).

10 Endarterectomy for asymptomatic carotid artery stenosis. Executive committee for the asymptomatic carotid atherosclerosis study. *JAMA* 273(18), 1421–1428 (1995).

11 Halliday A, Mansfield A, Marro J *et al.* Prevention of disabling and fatal strokes by successful carotid endarterectomy in patients without recent neurological symptoms: randomised controlled trial. *Lancet* 363(9420), 1491–1502 (2004).

12 Ryan TJ. The coronary angiogram and its seminal contributions to cardiovascular medicine over five decades. *Circulation* 106(6), 752 (2002).

13 Little W, Constantinescu M, Applegate R *et al.* Can coronary angiography predict the site of a subsequent myocardial infarction in patients with mild-to-moderate coronary artery disease? *Circulation* 78(5), 1157 (1988).

14 Nissen SE. Application of intravascular ultrasound to characterize coronary artery disease and assess the progression or regression of atherosclerosis. *Am. J. Cardiol.* 89(4A), 24B–31B (2002).

15 Garcia-Garcia HM, Mintz GS, Lerman A *et al.* Tissue characterisation using intravascular radiofrequency data analysis: recommendations for acquisition, analysis, interpretation and reporting. *EuroIntervention* 5(2), 177–189 (2009).

16 Moore M, Spencer T, Salter D *et al.* Characterisation of coronary atherosclerotic morphology by spectral analysis of

radiofrequency signal: *in vitro* intravascular ultrasound study with histological and radiological validation. *Heart* 79(5), 459–467 (1998).

17 Nair A, Kuban BD, Tuzcu EM *et al.* Coronary plaque classification with intravascular ultrasound radiofrequency data analysis. *Circulation* 106(17), 2200–2206 (2002).

18 Nasu K, Tsuchikane E, Katoh O *et al.* Accuracy of *in vivo* coronary plaque morphology assessment: a validation study of *in vivo* virtual histology compared with *in vitro* histopathology. *J. Am. Coll. Cardiol.* 47(12), 2405–2412 (2006).

19 Prati F, Arbustini E, Labellarte A *et al.* Correlation between high frequency intravascular ultrasound and histomorphology in human coronary arteries. *Heart* 85(5), 567 (2001).

20 Murashige A, Hiro T, Fujii T *et al.* Detection of lipid-laden atherosclerotic plaque by wavelet analysis of radiofrequency intravascular ultrasound signals: *in vitro* validation and preliminary *in vivo* application. *J. Am. Coll. Cardiol.* 45(12), 1954 (2005).

21 Kostamaa H, Donovan J, Kasaoka S *et al.* Calcified plaque cross-sectional area in human arteries: correlation between intravascular ultrasound and undecalcified histology. *Am. Heart J.* 137(3), 482–488 (1999).

22 Thim T, Hagensen MK, Wallace-Bradley D *et al.* Unreliable assessment of necrotic core by virtual histology intravascular ultrasound in porcine coronary artery disease. *Circ. Cardiovasc. Imaging* 3(4), 384–391 (2010).

23 Rodriguez-Granillo GA, Garcia-Garcia HM, Mc Fadden EP *et al. In vivo* intravascular ultrasound-derived thin-cap fibroatheroma detection using ultrasound radiofrequency data analysis. *J. Am. Coll. Cardiol.* 46(11), 2038–2042 (2005).

24 Schoenhagen P, Stone GW, Nissen SE *et al.* Coronary plaque morphology and frequency of ulceration distant from culprit lesions in patients with unstable and stable presentation. *Arterioscler. Thromb. Vasc. Biol.* 23(10), 1895–1900 (2003).

25 Kotani J, Mintz GS, Castagna MT *et al.* Intravascular ultrasound analysis of infarct-related and noninfarct-related arteries in patients who presented with an acute myocardial infarction. *Circulation* 107(23), 2889–2893 (2003).

26 Mintz GS, Nissen SE, Anderson WD *et al.* American College of Cardiology clinical expert consensus document on standards for acquisition, measurement and reporting of intravascular ultrasound studies (IVUS). A report of the American College of Cardiology Task Force on clinical expert consensus documents. *J. Am. Coll. Cardiol.* 37(5), 1478–1492 (2001).

27 Lipton M, Higgins C, Farmer D *et al.* Cardiac imaging with a high-speed cine-CT scanner: preliminary results. *Radiology* 152(3), 579 (1984).

28 Agatston AS, Janowitz WR, Hildner FJ *et al.* Quantification of coronary artery calcium using ultrafast computed tomography. *J. Am. Coll. Cardiol.* 15(4), 827–832 (1990).

29 Rist C, Johnson TR, Müller-Starck J *et al.* Noninvasive coronary angiography using dual-source computed tomography in patients with atrial fibrillation. *Invest. Radiol.* 44(3), 159 (2009).

30 Mowatt G, Cummins E, Waugh N *et al.* Systematic review of the clinical effectiveness and cost-effectiveness of 64-slice or higher computed tomography angiography as an alternative to invasive coronary angiography in the investigation of coronary artery disease. *Health Technol. Assess.* 12(17), iii–iv, ix–143 (2008).

31 Achenbach S, Ropers D, Kuettner A *et al.* Contrast-enhanced coronary artery visualization by dual-source computed tomography-initial experience. *E. J. Radiol.* 57(3), 331–335 (2006).

32 Ropers U, Ropers D, Pflederer T *et al.* Influence of heart rate on the diagnostic accuracy of dual-source computed tomography coronary angiography. *J. Am. Coll. Cardiol.* 50(25), 2393–2398 (2007).

33 Achenbach S, Goroll T, Seltmann M *et al.* Detection of coronary artery stenoses by low-dose, prospectively ECG-triggered, high-pitch spiral coronary CT angiography. *JACC Cardiovasc. Imaging* 4(4), 328–337 (2011).

34 Nikolaou K, Becker CR, Muders M *et al.* Multidetector-row computed tomography and magnetic resonance imaging of atherosclerotic lesions in human *ex vivo* coronary arteries. *Atherosclerosis* 174(2), 243–252 (2004).

35 Ferencik M, Chan RC, Achenbach S *et al.* Arterial wall imaging: evaluation with 16-section multidetector CT in blood vessel phantoms and *ex vivo* coronary arteries. *Radiology* 240(3), 708–716 (2006).

36 Horiguchi J, Fujioka C, Kiguchi M *et al.* Soft and intermediate plaques in coronary arteries: how accurately can we measure CT attenuation using 64-MDCT? *Am. J. Roentgenol.* 189(4), 981–988 (2007).

37 Achenbach S, Moselewski F, Ropers D *et al.* Detection of calcified and noncalcified coronary atherosclerotic plaque by contrast-enhanced, submillimeter multidetector spiral computed tomography: a segment-based comparison with intravascular ultrasound. *Circulation* 109(1), 14–17 (2004).

38 Leber AW, Knez A, Becker A *et al.* Accuracy of multidetector spiral computed tomography in identifying and differentiating the composition of coronary atherosclerotic plaques: a comparative study with intracoronary ultrasound. *J. Am. Coll. Cardiol.* 43(7), 1241–1247 (2004).

39 Leber AW, Becker A, Knez A *et al.* Accuracy of 64-slice computed tomography to classify and quantify plaque volumes in the proximal coronary system: a comparative study using intravascular ultrasound. *J. Am. Coll. Cardiol.* 47(3), 672–677 (2006).

40 Rasouli ML, Shavelle DM, French WJ *et al.* Assessment of coronary plaque morphology by contrast-enhanced computed tomographic angiography: comparison with intravascular ultrasound. *Coron. Artery Dis.* 17(4), 359–364 (2006).

41 Pohle K, Achenbach S, Macneill B *et al.* Characterization of noncalcified coronary atherosclerotic plaque by multidetector row CT: comparison to IVUS. *Atherosclerosis* 190(1), 174–180 (2007).

42 Sun J, Zhang Z, Lu B *et al.* Identification and quantification of coronary atherosclerotic plaques: a comparison of 64-MDCT and intravascular ultrasound. *Am. J. Roentgenol.* 190(3), 748 (2008).

43 De Weert TT, Ouhlous M, Meijering E *et al.* *In vivo* characterization and quantification of atherosclerotic carotid plaque components with multidetector computed tomography and histopathological correlation. *Arterioscler. Thromb. Vasc. Biol.* 26(10), 2366–2372 (2006).

44 Pundziute G, Schuijf JD, Jukema JW *et al.* Head-to-head comparison of coronary plaque evaluation between multislice computed tomography and intravascular ultrasound radiofrequency data analysis. *JACC Cardiovasc. Interv.* 1(2), 176–182 (2008).

45 Van Velzen JE, Schuijf JD, De Graaf FR *et al.* Plaque type and composition as evaluated noninvasively by MSCT angiography and invasively by VH IVUS in relation to the degree of stenosis. *Heart* 95(24), 1990–1996 (2009).

46 Funada R, Oikawa Y, Yajima J *et al.* The potential of RF backscattered IVUS data and multidetector-row computed tomography images for tissue characterization of human coronary atherosclerotic plaques. *Int. J. Cardiovasc. Imaging* 25(5), 471–478 (2009).

47 Pedrazzini GB, D'angeli I, Vassalli G *et al.* Assessment of coronary stenosis, plaque burden and remodeling by multidetector computed tomography in patients referred for

suspected coronary artery disease. *J. Cardiovasc. Med. (Hagerstown)* 12(2), 122–130 (2011).

48 Brenner DJ, Hall EJ. Computed tomography-an increasing source of radiation exposure. *N. Engl. J. Med.* 357(22), 2277–2284 (2007).

49 Smith-Bindman R, Lipson J, Marcus R *et al.* Radiation dose associated with common computed tomography examinations and the associated lifetime attributable risk of cancer. *Arch. Intern. Med.* 169(22), 2078–2086 (2009).

50 Achenbach S, Marwan M, Ropers D *et al.* Coronary computed tomography angiography with a consistent dose below 1 mSv using prospectively electrocardiogram-triggered high-pitch spiral acquisition. *Eur. Heart J.* 31(3), 340–346 (2010).

51 Boll DT, Merkle EM, Paulson EK *et al.* Calcified vascular plaque specimens: assessment with cardiac dual-energy multidetector CT in anthropomorphically moving heart phantom. *Radiology* 249(1), 119–126 (2008).

52 Hyafil F, Cornily JC, Rudd JH *et al.* Quantification of inflammation within rabbit atherosclerotic plaques using the macrophage-specific CT contrast agent N1177: a comparison with ^{18}F-FDG PET/CT and histology. *J. Nucl. Med.* 50(6), 959 (2009).

53 Hyafil F, Cornily JC, Feig JE *et al.* Noninvasive detection of macrophages using a nanoparticulate contrast agent for computed tomography. *Nature Med.* 13(5), 636–641 (2007).

54 Saam T, Hatsukami TS, Takaya N *et al.* The vulnerable, or high-risk, atherosclerotic plaque: noninvasive MR imaging for characterization and assessment. *Radiology* 244(1), 64–77 (2007).

55 Underhill HR, Hatsukami TS, Fayad ZA *et al.* MRI of carotid atherosclerosis: clinical implications and future directions. *Nat. Rev. Cardiol.* 7(3), 165–173 (2010).

56 Toussaint JF, Lamuraglia GM, Southern JF *et al.* Magnetic resonance images lipid, fibrous, calcified, hemorrhagic, and thrombotic components of human atherosclerosis *in vivo*. *Circulation* 94(5), 932–938 (1996).

57 Shinnar M, Fallon JT, Wehrli S *et al.* The diagnostic accuracy of *ex vivo* MRI for human atherosclerotic plaque characterization. *Arterioscler. Thromb. Vasc. Biol.* 19(11), 2756–2761 (1999).

58 Trivedi RA, U-King-Im J, Graves MJ *et al.* Multisequence *in vivo* MRI can quantify fibrous cap and lipid core components in human carotid atherosclerotic plaques. *Eur. J. Vasc. Endovasc. Surg.* 28(2), 207–213 (2004).

59 Saam T, Ferguson MS, Yarnykh VL *et al.* Quantitative evaluation of carotid plaque composition by *in vivo* MRI. *Arterioscler. Thromb. Vasc. Biol.* 25(1), 234–239 (2005).

60 Cai JM, Hatsukami TS, Ferguson MS *et al.* Classification of human carotid atherosclerotic lesions with *in vivo* multicontrast magnetic resonance imaging. *Circulation* 106(11), 1368–1373 (2002).

61 Chu B, Kampschulte A, Ferguson MS *et al.* Hemorrhage in the atherosclerotic carotid plaque: a high-resolution MRI study. *Stroke* 35(5), 1079–1084 (2004).

62 Kampschulte A, Ferguson MS, Kerwin WS *et al.* Differentiation of intraplaque versus juxtaluminal hemorrhage/thrombus in advanced human carotid atherosclerotic lesions by *in vivo* magnetic resonance imaging. *Circulation* 110(20), 3239–3244 (2004).

63 Ota H, Yarnykh VL, Ferguson MS *et al.* Carotid intraplaque hemorrhage imaging at 3.0-T MR imaging: comparison of the diagnostic performance of three T1-weighted sequences. *Radiology* 254(2), 551–563 (2010).

64 Hatsukami TS, Ross R, Polissar NL *et al.* Visualization of fibrous cap thickness and rupture in human atherosclerotic carotid plaque *in vivo* with high-resolution magnetic resonance imaging. *Circulation* 102(9), 959–964 (2000).

65 Cai J, Hatsukami TS, Ferguson MS *et al.* *In vivo* quantitative measurement of intact fibrous cap and lipid-rich necrotic core size in atherosclerotic carotid plaque: comparison of high-resolution, contrast-enhanced magnetic resonance imaging and histology. *Circulation* 112(22), 3437–3444 (2005).

66 Koktzoglou I, Chung YC, Mani V *et al.* Multislice dark-blood carotid artery wall imaging: a 1.5T and 3T comparison. *J. Magn. Reson. Imaging* 23(5), 699–705 (2006).

67 Saam T, Raya JG, Cyran CC *et al.* High resolution carotid black-blood 3T MR with parallel imaging and dedicated 4-channel surface coils. *J. Cardiovasc. Magn. Reson.* 11, 41 (2009).

68 Ota H, Reeves MJ, Zhu DC *et al.* Sex differences in patients with asymptomatic carotid atherosclerotic plaque: *in vivo* 3.0-T magnetic resonance study. *Stroke* 41(8), 1630–1635 (2010).

69 Parmar JP, Rogers WJ, Mugler JP *et al.* Magnetic resonance imaging of carotid atherosclerotic plaque in clinically suspected acute transient ischemic attack and acute ischemic stroke. *Circulation* 122(20), 2031–2038 (2010).

70 Boussel L, Arora S, Rapp J *et al.* Atherosclerotic plaque progression in carotid arteries: monitoring with high-spatial-resolution MR imaging-multicenter trial. *Radiology* 252(3), 789–796 (2009).

71 Underhill HR, Yarnykh VL, Hatsukami TS *et al.* Carotid plaque morphology and composition: initial comparison between 1.5- and 3.0-T magnetic field strengths. *Radiology* 248(2), 550–560 (2008).

72 Fayad ZA, Fuster V, Fallon JT *et al.* Noninvasive *in vivo* human coronary artery lumen and wall imaging using black-blood magnetic resonance imaging. *Circulation* 102(5), 506–510 (2000).

73 Botnar RM, Stuber M, Kissinger KV *et al.* Noninvasive coronary vessel wall and plaque imaging with magnetic resonance imaging. *Circulation* 102(21), 2582–2587 (2000).

74 Corti R, Fuster V. Imaging of atherosclerosis: magnetic resonance imaging. *Eur Heart J*, (2011).

75 Tanaka A, Kawasaki T, Noguchi T *et al.* Hyperintense plaque with noncontrast T1-weighted magnetic resonance coronary plaque imaging leading to acute coronary syndrome. *Circulation* 120(23), 2400–2401 (2009).

76 Tahara N, Imaizumi T, Virmani R *et al.* Clinical feasibility of molecular imaging of plaque inflammation in atherosclerosis. *J. Nucl. Med.* 50(3), 331–334 (2009).

77 Langer HF, Haubner R, Pichler BJ *et al.* Radionuclide imaging: a molecular key to the atherosclerotic plaque. *J. Am. Coll. Cardiol.* 52(1), 1–12 (2008).

78 Tawakol A, Migrino RQ, Bashian GG *et al.* *In vivo* ^{18}F-fluorodeoxyglucose positron emission tomography imaging provides a noninvasive measure of carotid plaque inflammation in patients. *J. Am. Coll. Cardiol.* 48(9), 1818–1824 (2006).

79 Tahara N, Kai H, Yamagishi S *et al.* Vascular inflammation evaluated by [^{18}F]-fluorodeoxyglucose positron emission tomography is associated with the metabolic syndrome. *J. Am. Coll. Cardiol.* 49(14), 1533–1539 (2007).

80 Saam T, Rominger A, Wolpers S *et al.* Association of inflammation of the left anterior descending coronary artery with cardiovascular risk factors, plaque burden and pericardial fat volume: a PET/CT study. *Eur. J. Nucl. Med. Mol. Imaging* 37(6), 1203–1212 (2010).

81 Rudd JH, Myers KS, Bansilal S *et al.* (18) Fluorodeoxyglucose positron emission tomography imaging of atherosclerotic plaque inflammation is highly reproducible: implications for atherosclerosis therapy trials. *J. Am. Coll. Cardiol.* 50(9), 892–896 (2007).

82 Tahara N, Kai H, Ishibashi M *et al.* Simvastatin attenuates plaque inflammation: evaluation by fluorodeoxyglucose positron emission tomography. *J. Am. Coll. Cardiol.* 48(9), 1825–1831 (2006).

83 Kolodgie FD, Petrov A, Virmani R *et al.* Targeting of apoptotic macrophages and experimental atheroma with radiolabeled annexin V: a technique with potential for noninvasive imaging of vulnerable plaque. *Circulation* 108(25), 3134–3139 (2003).

84 Huang B, Law MW, Khong PL. Whole-body PET/CT scanning: estimation of radiation dose and cancer risk. *Radiology* 251(1), 166–174 (2009).

85 Saam T, Underhill HR, Chu B *et al.* Prevalence of American Heart Association type VI carotid atherosclerotic lesions identified by magnetic resonance imaging for different levels of stenosis as measured by duplex ultrasound. *J. Am. Coll. Cardiol.* 51(10), 1014–1021 (2008).

86 Pijls NH, Fearon WF, Tonino PA *et al.* Fractional flow reserve versus angiography for guiding percutaneous coronary intervention in patients with multivessel coronary artery disease: 2-year follow-up of the FAME study. *J. Am. Coll. Cardiol.* 56(3), 177–184 (2010).

87 Boden W, O'Rourke R, Teo K. Optimal medical therapy with or without PCI for stable coronary disease (COURAGE). *N. Engl. J. Med.* 356(15), 1503–1516 (2007).

88 Georgiou D, Budoff MJ, Kaufer E *et al.* Screening patients with chest pain in the emergency department using electron beam tomography: a follow-up study. *J. Am. Coll. Cardiol.* 38(1), 105–110 (2001).

89 Bild DE, Burke G, Folsom AR *et al.* Coronary calcium as a predictor of coronary events in four racial or ethnic groups. *N. Engl. J. Med.* 358, 1336–1345 (2008).

90 Lamonte MJ, Fitzgerald SJ, Church TS *et al.* Coronary artery calcium score and coronary heart disease events in a large cohort of asymptomatic men and women. *Am. J. Epidemiol.* 162(5), 421 (2005).

91 Taylor AJ, Bindeman J, Feuerstein I *et al.* Coronary calcium independently predicts incident premature coronary heart disease over measured cardiovascular risk factors: mean 3-year outcomes in the prospective army coronary calcium (PACC) project. *J. Am. Coll. Cardiol.* 46(5), 807–814 (2005).

92 Vliegenthart R, Oudkerk M, Hofman A *et al.* Coronary calcification improves cardiovascular risk prediction in the elderly. *Circulation* 112(4), 572 (2005).

93 Ahmadi N, Hajsadeghi F, Blumenthal RS *et al.* Mortality in individuals without known coronary artery disease but with discordance between the Framingham risk score and coronary artery calcium. *Am. J. Cardiol.* 107(6), 799–804 (2011).

94 Motoyama S, Sarai M, Harigaya H *et al.* Computed tomographic angiography characteristics of atherosclerotic plaques subsequently resulting in acute coronary syndrome. *J. Am. Coll. Cardiol.* 54(1), 49–57 (2009).

95 Sano K, Kawasaki M, Ishihara Y *et al.* Assessment of vulnerable plaques causing acute coronary syndrome using integrated backscatter intravascular ultrasound. *J. Am. Coll. Cardiol.* 47(4), 734–741 (2006).

96 Yamagishi M, Terashima M, Awano K *et al.* Morphology of vulnerable coronary plaque: insights from follow-up of patients examined by intravascular ultrasound before an acute coronary syndrome. *J. Am. Coll. Cardiol.* 35(1), 106–111 (2000).

97 Hoffmann U, Moselewski F, Nieman K *et al.* Noninvasive assessment of plaque morphology and composition in culprit and stable lesions in acute coronary syndrome and stable lesions in stable angina by multidetector computed tomography. *J. Am. Coll. Cardiol.* 47(8), 1655–1662 (2006).

98 Madder RD, Chinnaiyan KM, Marandici AM *et al.* Features of disrupted plaques by coronary CT angiography: correlates with invasively-proven complex lesions. *Circ. Imaging* DOI: 10.1161/CIRCIMAGING.110.957282 (2011).

99 Pflederer T, Marwan M, Schepis T *et al.* Characterization of culprit lesions in acute coronary syndromes using coronary dual-source CT angiography. *Atherosclerosis* 211(2), 437–444 (2010).

100 Fujii K, Kobayashi Y, Mintz GS *et al.* Intravascular ultrasound assessment of ulcerated ruptured plaques: a comparison of culprit and nonculprit lesions of patients with acute coronary syndromes and lesions in patients without acute coronary syndromes. *Circulation* 108(20), 2473–2478 (2003).

101 Motoyama S, Kondo T, Sarai M *et al.* Multislice computed tomographic characteristics of coronary lesions in acute coronary syndromes. *J. Am. Coll. Cardiol.* 50(4), 319–326 (2007).

102 Kroner ES, Van Velzen JE, Boogers MJ *et al.* Positive remodeling on coronary computed tomography as a marker for plaque vulnerability on virtual histology intravascular ultrasound. *Am. J. Cardiol.* 107(12), 1725–1729 (2011).

103 Schoenhagen P, Ziada KM, Kapadia SR, *et al.* Extent and direction of arterial remodeling in stable versus unstable coronary syndromes: an intravascular ultrasound study. *Circulation* 101(6), 598–603 (2000).

104 Nakamura M, Nishikawa H, Mukai S *et al.* Impact of coronary artery remodeling on clinical presentation of coronary artery disease: an intravascular ultrasound study. *J. Am. Coll. Cardiol.* 37(1), 63–69 (2001).

105 Von Birgelen C, Klinkhart W, Mintz GS *et al.* Plaque distribution and vascular remodeling of ruptured and nonruptured coronary plaques in the same vessel: an intravascular ultrasound study *in vivo*. *J. Am. Coll. Cardiol.* 37(7), 1864–1870 (2001).

106 Ehara S, Kobayashi Y, Yoshiyama M *et al.* Spotty calcification typifies the culprit plaque in patients with acute myocardial infarction: an intravascular ultrasound study. *Circulation* 110(22), 3424–3429 (2004).

107 Kitagawa T, Yamamoto H, Horiguchi J *et al.* Characterization of noncalcified coronary plaques and identification of culprit lesions in patients with acute coronary syndrome by 64-slice computed tomography. *JACC Cardiovasc. Imaging* 2(2), 153–160 (2009).

108 Huang WC, Wu MT, Chiou KR *et al.* Assessing culprit lesions and active complex lesions in patients with early acute myocardial infarction by multidetector computed tomography. *Circ. J.* 72(11), 1806–1813 (2008).

109 Missel E, Mintz GS, Carlier SG *et al.* Necrotic core and its ratio to dense calcium are predictors of high-risk non-ST-elevation acute coronary syndrome. *Am. J. Cardiol.* 101(5), 573–578 (2008).

110 Hong MK, Mintz GS, Lee CW *et al.* A three-vessel virtual histology intravascular ultrasound analysis of frequency and distribution of thin-cap fibroatheromas in patients with acute coronary syndrome or stable angina pectoris. *Am. J. Cardiol.* 101(5), 568–572 (2008).

111 Surmely JF, Nasu K, Fujita H *et al.* Association of coronary plaque composition and arterial remodelling: a virtual histology analysis by intravascular ultrasound. *Heart* 93(8), 928–932 (2007).

112 Takaoka H, Ishibashi I, Uehara M *et al.* Comparison of image characteristics of plaques in culprit coronary arteries by 64 slice CT and intravascular ultrasound in acute coronary syndromes. *Int. J. Cardiol.* DOI: 10.1016/j.ijcard.2011.04.014 (2011) (Epub ahead of print).

113 Murphy RE, Moody AR, Morgan PS *et al.* Prevalence of complicated carotid atheroma as detected by magnetic resonance direct thrombus imaging in patients with suspected carotid artery stenosis and previous acute cerebral ischemia. *Circulation* 107(24), 3053–3058 (2003).

114 Takaya N, Yuan C, Chu B *et al.* Association between carotid plaque characteristics and subsequent ischemic cerebrovascular events: a prospective assessment with MRI--initial results. *Stroke* 37(3), 818–823 (2006).

115 Altaf N, Daniels L, Morgan PS *et al.* Detection of intraplaque hemorrhage by magnetic resonance imaging in symptomatic patients with mild to moderate carotid stenosis predicts recurrent neurological events. *J. Vasc. Surg.* 47(2), 337–342 (2008).

116 Takaya N, Yuan C, Chu B *et al.* Presence of intraplaque hemorrhage stimulates progression of carotid atherosclerotic plaques: a high-resolution magnetic resonance imaging study. *Circulation* 111(21), 2768–2775 (2005).

117 Kolodgie FD, Gold HK, Burke AP *et al.*: Intraplaque hemorrhage and progression of coronary atheroma. *N. Engl. J. Med.* 349(24), 2316–2325 (2003).

118 Rudd JH, Warburton EA, Fryer TD *et al.* Imaging atherosclerotic plaque inflammation with [^{18}F]-fluorodeoxyglucose positron emission tomography. *Circulation* 105(23), 2708–2711 (2002).

119 Kwee RM, Truijman MT, Mess WH *et al.* Potential of integrated [^{18}F] fluorodeoxyglucose positron-emission tomography/CT in identifying vulnerable carotid plaques. *Am. J. Neuroradiol.* 32(5), 950–954 (2011).

120 Rominger A, Saam T, Wolpers S *et al.* ^{18}F-FDG PET/CT identifies patients at risk for future vascular events in an otherwise asymptomatic cohort with neoplastic disease. *J. Nucl. Med.* 50(10), 1611–1620 (2009).

121 Altaf N, Beech A, Goode SD *et al.* Carotid intraplaque hemorrhage detected by magnetic resonance imaging predicts embolization during carotid endarterectomy. *J. Vasc. Surg.* 46(1), 31–36 (2007).

122 Yoshimura S, Kawasaki M, Asano T *et al.* High intensity signal on time of flight MR angiography indicates carotid plaques at high risk for cerebral embolism after stenting. *Stroke* DOI: 10.1161/STROKEAHA. 111.615708 (2011) (Epub ahead of print).

123 Yamada K, Kawasaki M, Yoshimura S *et al.* Prediction of silent ischemic lesions after carotid artery stenting using integrated backscatter ultrasound and magnetic resonance imaging. *Atherosclerosis* 208(1), 161–166 (2010).

124 Ramcharitar S, Gonzalo N, Van Geuns RJ *et al.* First case of stenting of a vulnerable plaque in the SECRITT I trial-the dawn of a new era? *Nat. Rev. Cardiol.* 6(5), 374–378 (2009).

125 Muntendam P, Mccall C, Sanz J *et al.* The BioImage Study: novel approaches to risk assessment in the primary prevention of atherosclerotic cardiovascular disease--study design and objectives. *Am. Heart J.* 160(1), 49–57 e1 (2010).

126 Vancraeynest D, Pasquet A, Roelants V *et al.* Imaging the vulnerable plaque. *J. Am. Coll. Cardiol.* 57(20), 1961–1979 (2011).

127 Saam T, Cai J, Ma L *et al.* Comparison of symptomatic and asymptomatic atherosclerotic carotid plaque features with *in vivo* MR imaging. *Radiology* 240(2), 464–472 (2006).

128 Rogers IS, Nasir K, Figueroa AL *et al.* Feasibility of FDG imaging of the coronary arteries: comparison between acute coronary syndrome and stable angina. *JACC Cardiovasc. Imaging* 3(4), 388–397 (2010).

129 Detrano R, Guerci AD, Carr JJ *et al.* Coronary calcium as a predictor of coronary events in four racial or ethnic groups. *N. Engl. J. Med.* 358(13), 1336–1345 (2008).